

Article

Leading Singularities in Higher-Derivative Yang–Mills Theory and Quadratic Gravity

Gabriel Menezes 

Departamento de Física, Universidade Federal Rural do Rio de Janeiro, Seropédica 23897-000, RJ, Brazil; gabrielmenezes@ufrj.br

Abstract: In this work, we explore general leading singularities of one-loop amplitudes in higher-derivative Yang–Mills and quadratic gravity. These theories are known to possess propagators which contain quadratic and quartic momentum dependence, which leads to the presence of an unstable ghostlike resonance. However, unitarity cuts are not to be taken through unstable particles and therefore unitarity is still satisfied. On the other hand, this could engender issues when calculating leading singularities which are generalizations of unitarity cuts. Nevertheless, we will show with explicit examples how leading singularities are still well defined and accordingly they are able to capture relevant information on the analytic structure of amplitudes in such higher-derivative theories. We discuss some simple one-loop amplitudes which clarify these features.

Keywords: scattering amplitudes; quadratic gravity; higher-derivative theories



Citation: Menezes, G. Leading Singularities in Higher-Derivative Yang–Mills Theory and Quadratic Gravity. *Universe* **2022**, *8*, 326. <https://doi.org/10.3390/universe8060326>

Academic Editors: Lisa Glaser, Alessia Platania and Sebastian Steinhaus

Received: 10 May 2022

Accepted: 8 June 2022

Published: 10 June 2022

Publisher's Note: MDPI stays neutral with regard to jurisdictional claims in published maps and institutional affiliations.



Copyright: © 2022 by the author. Licensee MDPI, Basel, Switzerland. This article is an open access article distributed under the terms and conditions of the Creative Commons Attribution (CC BY) license (<https://creativecommons.org/licenses/by/4.0/>).

1. Introduction

The analytic properties of scattering amplitudes have been meticulously examined in the literature [1–12]. The idea is to regard the amplitude as an analytic function of kinematical invariants—and physical input would be needed to ascertain all associated singularities. Several decades ago, this project developed into the ambitious expectation that an adequate understanding of the structure of its singularities would enable one to determine the S-matrix itself and, as a consequence, one would obtain a deep insight of all the interactions involved. However, this program has proven to be a formidable task. In any case, such investigations have unveiled the intricate analytic structure that amplitudes may have in perturbation theory. Indeed, at the loop level, Feynman diagrams enjoy a configuration that is rather involved consisting of nested branch cuts. This complicated structure gets even more complex when one goes to higher orders in perturbation theory. This non-trivial analytic structure can be envisaged when assuming unitarity; that is, imposing the generalized optical theorem should be satisfied. It is the assumption of this constraint that makes it possible to relate the discontinuity of an amplitude to the exchange of on-shell states among sets of external particles. One-particle exchange is associated with the existence of poles, whereas a two-particle exchange indicates the presence of a branch cut.

The discontinuity across a pole is the residue of the associated holomorphic function at such a pole. Often we discuss discontinuities in a given channel from the perspective of the so-called cutting rules [13,14], which basically deals with two-particle exchanges. In summary, we use such rules to compute the imaginary part of loop amplitudes, which furnishes their discontinuities. An alternative interpretation is to conceive unitarity cuts as residues of the amplitude; for instance, for two-particle exchange we take two propagators $1/(L_1^2 - m_1^2)$ and $1/(L_2^2 - m_2^2)$ (they can also be massless), then integrate over contours that surround the poles $L_i^2 - m_i^2 = 0$ in the associated complex planes. This amounts to removing the principal part of the propagator, keeping only its imaginary part given by the associated delta functions $\delta(L_i^2 - m_i^2)$, in compliance with the fact that imaginary parts of

loop amplitudes correspond to intermediate particles going on-shell. In this regard, the hope alluded to earlier was partially fulfilled some time ago, when it was shown that the use of branch cut singularities could be a powerful tool in the calculations of scattering amplitudes. This program has given birth to a solid framework which nowadays is known as the unitarity-based method [15–21]. This technique has since streamlined the evaluation of many loop amplitudes; at one-loop, the problem of computing amplitudes boils down to computing tree amplitudes—in many cases, we also need to calculate rational terms.

On the other hand, discontinuities in a given physical channel also possess by themselves an elaborate analytic structure. Hence, the cutting process can be repeated over and over again, which leads to what became known as generalized unitarity constraints [2,22–50]¹. It did not take long for many authors to realize that this could also be useful in the evaluation of loop amplitudes. In the method of generalized unitarity, the aim is to find an integrand that could reproduce all possible unitarity cuts. In the process, one may require the integrand to reproduce each of the cut solutions independently. The resulting value for the cut calculated on each solution is called a leading singularity [2–6,51–54]. This technique is reminiscent of the so-called maximal-cut method in the sense that it also requires the cutting of a maximal (or near-maximal) number of propagators. To put it simply, leading singularities are generalizations of standard unitarity cuts. The latter evaluates discontinuities across co-dimension one branch cuts; leading singularities are associated with singularities of the highest possible co-dimension and are evaluated as multidimensional residues, possessing support outside the physical region of integration.

Leading singularities comprise a powerful technique to compute amplitudes. Whereas standard unitarity cuts might have divergences, leading singularities are calculated using compact contours and are hence finite. Moreover, leading singularities encompass physical states and are gauge-invariant, a property also enjoyed by standard unitarity cuts. These features make them useful quantities to employ in the study of general theories. For instance, it was shown that it is also a valuable contrivance when addressing classical scattering and as a consequence it can be helpful in the calculation of many important classical observables, reducing many calculations which could be very complicated within the framework of general relativity [55–58]. In this work, we wish to show that they can also be useful in the study of the analytic properties of scattering amplitudes in Lee–Wick-type theories. This kind of higher-derivative theory was shown to be unitary despite the presence of an unstable ghostlike resonance [59]. We are particularly interested in a higher-derivative version of the Yang–Mills theory and also quadratic gravity. The latter still constitutes a potential UV completion for quantum gravity [60,61]. We will study one-loop scattering of gluons and gravitons as well as scattering of matter particles in such higher-derivative theories. We remark that leading singularities in cubic theories of gravity were already considered in [62,63].

Even though unitarity in theories with unstable particles is only assured when unitarity cuts are not taken through unstable propagators [59,64–68], recently it was argued that the unitarity method still works for loop amplitudes containing resonances [69]. This implies that the leading-singularity technique is also available to approach amplitudes in such theories. On the other hand, causality is violated on microscopic scales of order for the width of the resonance [70–76]. This is a consequence of the fact that the poles associated with such unusual resonances are on the physical sheet of the analytic continuation of the scattering amplitude; therefore, the resummed propagators do not satisfy the usual analyticity properties. In the calculation of one-loop Feynman diagrams using standard methods (or when proving the cutting rules directly from Feynman diagrams), this demands the usage of a deformed contour, the Lee–Wick contour [59,70,73], perhaps together with some additional prescription, known in the literature as the Cutkosky–Landshoff–Olive–Polkinghorn (CLOP) prescription [77]. Even though important recent efforts were made towards a better understanding of the analytic properties of amplitudes of higher-derivative theories [78–83], modern tools were put in an application only recently [84–87]. Our investigation therefore furnishes a promising avenue for the comprehension of the analytic structure of loop am-

plitudes in higher-derivative Yang–Mills and quadratic gravity theories. Here, we will use units such that $\hbar = c = 1$. We take the Minkowski metric as $\eta_{\mu\nu} = \text{diag}(1, -1, -1, -1)$ and the Riemann curvature tensor given by $R^\lambda_{\mu\nu\kappa} = \partial_\kappa \Gamma^\lambda_{\mu\nu} + \Gamma^\eta_{\mu\nu} \Gamma^\lambda_{\kappa\eta} - (v \leftrightarrow \kappa)$.

2. Brief Review of Color–Kinematics Duality and Yang–Mills Amplitudes

In this section, we will give a brief review of an intriguing result involving Yang–Mills amplitudes which became known as the color–kinematics duality [88–111]. We will also list all important gauge-theory amplitudes that will be important in the calculations that follow.

Tree-level amplitudes of the Yang–Mills theory can be written as a sum over distinct trivalent diagrams [51]:

$$A_n = \sum_k \frac{c_k n_k}{s_k} \tag{1}$$

where s_k are inverse propagators (which could be massive), the c_k s are associated color factors and the numerators n_k are in general polynomials of Lorentz-invariant contractions of polarization vectors and momenta. When the color factors satisfy Jacobi identities such as

$$c_i + c_j + c_k = 0 \tag{2}$$

one can easily prove that the amplitude is invariant under generalized gauge transformations:

$$n_i \rightarrow n_i + s_i \Delta, \quad n_j \rightarrow n_j + s_j \Delta, \quad n_k \rightarrow n_k + s_k \Delta, \tag{3}$$

where Δ is an arbitrary function and s_i, s_j, s_k are inverse propagators not shared among the different diagrams associated with each of the above color factors. On the other hand, this also implies that such numerators are not, in general, gauge-invariant, despite the fact that the amplitude is. Moreover, the above color factors can also obey relations such as $c_i = -c_j$.

The so-called color–kinematics duality states that there exists at least one representation for gauge-theory amplitudes such that the numerators will satisfy identical algebraic properties as the corresponding color factors; that is,

$$n_i + n_j + n_k = 0 \tag{4}$$

and also, for instance, $n_i = -n_j$. The fact that such gauge-dependent numerators obey these relations has one direct important consequence: One can derive gauge-invariant homogeneous relations between color-ordered partial amplitudes [89]. These are the so-called BCJ amplitude relations.

A somewhat different perspective arises in gauge theories with higher-derivative operators in the Lagrangian. Here, we will be particularly interested in the higher-derivative Yang–Mills with a Lagrangian density given by [72,85,87]

$$M^2 \mathcal{L} = -\frac{M^2}{4} F^\alpha_{\mu\nu} F^{\alpha\mu\nu} + \frac{1}{2} D_\mu F^{\alpha\mu\nu} D_\lambda F^{\alpha\lambda}_\nu \tag{5}$$

where covariant-derivative in the adjoint representation reads

$$D^\mu F^\alpha_{\beta\gamma} = \partial^\mu F^\alpha_{\beta\gamma} + g f^{abc} A^{b\mu} F^\alpha_{\beta\gamma}. \tag{6}$$

As is well known, higher-derivative terms modify the propagation of particles in such a way that the associated propagator develops a massive contribution with wrong-sign residue. We can interpret such a massive term as a new degree of freedom of the theory, a ghost “particle” in itself, one carrying a different causal direction, as discussed in [74,76]. Such ghost particles were dubbed *Merlin modes* elsewhere [74,75]. Even though Merlin modes could give rise to major problems, it was proved that the theory is unitary [59] and possibly stable, at least in certain contexts [112,113]. These are consequences of the fact that the Merlin modes are unstable and hence they cannot appear in the asymptotic

spectrum. The possible drawback is that such theories predict causality violation for microscopic time scales. However, as the theory possesses unitary time evolution, one cannot verify paradoxes in experiments that involve normal particles in the asymptotic states—the theory may have unconventional acausal effects, but this feature does not seem to make it inconsistent.

We take the total gauge propagator in the form [87]

$$D_{\mu\nu}^{ab}(p) = -\frac{\delta^{ab}}{p^2} \left(\eta_{\mu\nu} - (1 - \zeta) \frac{p_\mu p_\nu}{p^2} \right) + \frac{\delta^{ab}}{p^2 - M^2 - iM\Gamma} \left(\eta_{\mu\nu} - \frac{p_\mu p_\nu}{M^2} \right). \tag{7}$$

Henceforth, we will consider the Feynman gauge, $\zeta = 1$. The second contribution is the Merlin propagator in the narrow-width approximation, with $\Gamma \ll M$ being the decay width of the Merlin particle. Recall that, in general, one should consider a resummed form for unstable propagators as perturbation theory breaks down in the resonance region. Observe the two unusual minus signs in this equation; the change in the two signs together implies that the imaginary part of the Merlin propagator is the same as a normal resonance, a feature of the utmost importance for unitarity to hold—and, as a result, the generalized unitarity method still makes sense in the applications for higher-derivative theories. In what follows, unless otherwise stated, the contribution of the width Γ will be left implicit in the Merlin propagators.

Concerning color–kinematics duality, it was shown in [87] that four-point amplitudes in such a theory still obey the duality, but with an unusual feature—the presence of quartic propagators renders the numerators in the amplitudes gauge-invariant and as a consequence color-ordered amplitudes will not display conventional BCJ relations. In this case, the amplitude representation we have derived is necessarily unique and color–kinematics duality is trivially satisfied.

We will now list some of the tree-level amplitudes of higher-derivative Yang–Mills theories that will be used in the considerations that will follow. Let us begin with the three-particle amplitude. As demonstrated in [85,87], three-particle amplitudes involving only physical gluons will not display contributions coming from higher-order derivative terms:

$$A_3^{(4)}[1^{h_1}, 2^{h_2}, 3^{h_3}] = M^2 A_3^{(2)}[1^{h_1}, 2^{h_2}, 3^{h_3}] \tag{8}$$

where the h_i s are different helicities of the gluons and the superscripts represent the four- and two-derivative theories. Square brackets for color-ordered gauge-theory amplitudes are used in order to make an explicit distinction from non-color-ordered amplitudes. A coefficient g/M^2 was also factored out. In particular, such gluon amplitudes are completely fixed by little group scaling and locality. We find that [51]

$$\begin{aligned} A_3^{(2)}[1^-, 2^-, 3^+] &= \frac{\langle 12 \rangle^3}{\langle 13 \rangle \langle 32 \rangle} \\ A_3^{(2)}[1^+, 2^+, 3^-] &= \frac{[12]^3}{[13][32]}. \end{aligned} \tag{9}$$

By employing BCFW recursion relations [114,115], one can show that the result (8) generalizes to an arbitrary number of gluons:

$$A_n^{(4)}[1^{h_1}, 2^{h_2}, 3^{h_3}, \dots, n^{h_n}] = M^2 A_n^{(2)}[1^{h_1}, 2^{h_2}, 3^{h_3}, \dots, n^{h_n}] \tag{10}$$

Furthermore, momentum conservation allows us to show that the three-particle on-shell amplitude involving a single Merlin particle vanishes [85,87]:

$$A_3^{(4)}(1^{h_1}, 2^{h_2}, 3^I) = 0, \tag{11}$$

which also can be generalized to

$$A_{n+1}^{(4)}(1^{h_1}, 2^{h_2}, \dots, n^{h_n}, k^{IJ}) = 0. \tag{12}$$

Observe that massive gauge bosons carry explicit $SU(2)$ little-group indices. In what follows, we will use instead a bold notation to suitably indicate symmetric combinations of $SU(2)$ little-group indices for massive spinors. For a pedagogical discussion of the formalism for massive spinors adopted in the present work, see [116–120].

Finally, the case with two Merlin particles is non-trivial; we find that [87,121]

$$\begin{aligned} A_3[1^+, \mathbf{2}, \mathbf{3}] &= \sqrt{2} \frac{\langle r|\mathbf{3}|1\rangle}{\langle r1\rangle} \langle \mathbf{32}\rangle^2 \\ A_3[1^-, \mathbf{2}, \mathbf{3}] &= \sqrt{2} \frac{[r|\mathbf{3}|1\rangle}{[1r]} [\mathbf{32}]^2. \end{aligned} \tag{13}$$

To complete our list of three-particle on-shell amplitudes, let us write down the results involving gluons or Merlins with two scalars. Actually the amplitudes have the same form—the difference relies on the polarization vectors. For gluons, which are massless, the three-point amplitudes for one positive-helicity gluon and two massive (complex) scalars of mass μ^2 read [122]

$$A_3^{\text{tree}}(\ell_{iA}^+, p^{a+}, \ell_{jB}^-) = g T_{ij}^a (\ell_A^\mu - \ell_B^\mu) \epsilon_\mu(p) = g T_{ij}^a \sqrt{2} \frac{\langle \bar{\zeta} | \ell_A | p \rangle}{\langle \bar{\zeta} p \rangle} \tag{14}$$

where T^a are $SU(N)$ generators in the fundamental representation, which satisfy

$$\begin{aligned} [T^a, T^b] &= i f^{abc} T^c \\ \text{Tr}[T^a T^b] &= \frac{1}{2} \delta^{ab} \end{aligned} \tag{15}$$

(f^{abc} are the structure constants) and $|\bar{\zeta}\rangle$ is an arbitrary reference spinor not proportional to $|p\rangle$. Now, for Merlins, which are massive, we obtain that [87]

$$A_3^{\text{tree}}(\ell_{iA}^+, \mathbf{p}^a, \ell_{jB}^-) = g T_{ij}^a (\ell_A^\mu - \ell_B^\mu) \epsilon_\mu(\mathbf{p}) = g T_{ij}^a \sqrt{2} \frac{\langle \mathbf{p} | \ell_A | \mathbf{p} \rangle}{M}. \tag{16}$$

Let us now move on to four-point amplitudes. In the situation involving only gluons, we have already noted that the amplitudes are essentially the same as in the pure Yang–Mills theory. In this case, non-vanishing color-ordered amplitudes are the so-called N^K MHV amplitudes, which contain $K + 2$ negative-helicity gluons and $n - K - 2$ positive-helicity gluons. The MHV and the anti-MHV amplitudes are given by the Parke–Taylor formula [123]:

$$\begin{aligned} A_n^{\text{MHV,tree}}[1^+, \dots, i^-, \dots, j^-, \dots, n^+] &= \frac{\langle ij\rangle^4}{\prod_{i=1}^n \langle i, i+1\rangle} \\ A_n^{\text{antiMHV,tree}}[1^-, \dots, i^+, \dots, j^+, \dots, n^-] &= \frac{[ij]^4}{\prod_{i=1}^n [i, i+1]} \end{aligned} \tag{17}$$

respectively, where $n + 1 \rightarrow 1$. The Parke–Taylor formula can be proved using the BCFW recursion relations.

Compton amplitudes involving Merlin particles were considered in detail in [87]. In particular, we are interested in the color-ordered amplitude $A_4[2, 1^+, 4^+, 3]$ with Merlins and gluons. Using BCFW recursion relations, one finds that [87,121]

$$A_4[2, 1^+, 4^+, 3] = 2M^4 \frac{[14]}{\langle 14\rangle} \frac{\langle \mathbf{32}\rangle^2}{(p_1 + p_2)^2 - M^2}. \tag{18}$$

The other Compton scattering amplitudes that will be used in the calculation of the associated leading singularities are the ones with two gauge particles and two massive fundamental scalars with mass m . The ones with gluons read [119,121,124]

$$\begin{aligned}
 A_4(\ell_{iA}, 1^{a+}, 2^{b-}, \ell_{jB}) &= -\frac{2g^2}{t} \left(\frac{T_{ik}^a T_{kj}^b}{2\ell_A \cdot p_1} + \frac{T_{ik}^b T_{kj}^a}{2\ell_A \cdot p_2} \right) \langle 2|\ell_A|1 \rangle^2 \\
 A_4(\ell_{iA}, 1^{a-}, 2^{b-}, \ell_{jB}) &= 2m^2 g^2 \frac{\langle 21 \rangle^2}{(p_1 + p_2)^2} \left[\frac{T_{ik}^a T_{lk}^b}{(\ell_A + p_1)^2 - m^2} + \frac{T_{ik}^b T_{kj}^a}{(\ell_A + p_2)^2 - m^2} \right].
 \end{aligned}
 \tag{19}$$

The associated reverse-helicity amplitudes can be obtained from those above by swapping angle and square brackets. In turn, the amplitude with external Merlins is given by [87]

$$\begin{aligned}
 A_4(\ell_{iA}, \mathbf{1}^a, \mathbf{2}^b, \ell_{jB}) &= 2g^2 T_{ik}^a T_{kj}^b \frac{\langle \mathbf{1}|\ell_A|\mathbf{1} \rangle \langle \mathbf{2}|\ell_B|\mathbf{2} \rangle}{M^2} \frac{1}{(\ell_A + p_1)^2 - m^2} + 2g^2 T_{ik}^b T_{kj}^a \frac{\langle \mathbf{1}|\ell_B|\mathbf{1} \rangle \langle \mathbf{2}|\ell_A|\mathbf{2} \rangle}{M^2} \frac{1}{(\ell_A + p_2)^2 - m^2} \\
 &- ig^2 f^{bac} T_{ij}^c \frac{2}{M^2} \left[\langle \mathbf{12} \rangle [\mathbf{21}] (\mathbf{1} - \mathbf{2}) \cdot \ell_A - \left(\langle \mathbf{1}|\ell_A|\mathbf{1} \rangle \langle \mathbf{2}|\mathbf{1}|\mathbf{2} \rangle - \langle \mathbf{2}|\ell_A|\mathbf{2} \rangle \langle \mathbf{1}|\mathbf{2}|\mathbf{1} \rangle \right) \right] \\
 &\times \left(\frac{1}{(p_1 + p_2)^2} - \frac{2}{(p_1 + p_2)^2 - M^2} \right) \\
 &+ g^2 \{T^a, T^b\}_{ij} \frac{\langle \mathbf{12} \rangle [\mathbf{21}]}{M^2}.
 \end{aligned}
 \tag{20}$$

The overall minus sign in front of the last term in the t -channel is a consequence of the ghost feature of the Merlin mode.

There is still one amplitude we need that was not calculated previously—this is the four-point amplitude with scalars, with a Merlin and a gluon as external states. In order to build up such a scattering amplitude, we will consider the contributions due to consistent factorization in all possible channels given the three-particle amplitudes. The residue in the s -channel is given by

$$\text{Res}_s = 2\sqrt{2} \frac{\langle \mathbf{1}|\ell_A|\mathbf{1} \rangle}{M} \ell_B^\mu \epsilon_\mu(2).
 \tag{21}$$

The residue in the u -channel is obtained by swapping the Merlin with the gluon. As amplitudes involving a single Merlin particle vanish, the residue in the t -channel presents us with only one possibility—the pole must come from the massive Merlin particle. Thus, the residue is given by the product of a three-point amplitude involving two scalars and a Merlin and with another three-point amplitude with two Merlins and a gluon²:

$$\begin{aligned}
 \text{Res}_t &= -M^2 \left[\eta_{\mu\nu} (p_1 - p_2)_\rho + \eta_{\nu\rho} (2p_2 + p_1)_\mu - \eta_{\rho\mu} (2p_1 + p_2)_\nu \right] \epsilon^{\mu IJ}(\mathbf{1}) \epsilon^\nu(2) \epsilon^{\rho MN}(\mathbf{p}) 2\ell_{A\alpha} [\epsilon_{MN}^\alpha(\mathbf{p})]^* \\
 &= 2M^2 \left[\eta_{\mu\nu} (p_1 - p_2)_\rho + \eta_{\nu\rho} (2p_2 + p_1)_\mu - \eta_{\rho\mu} (2p_1 + p_2)_\nu \right] \epsilon^{\mu IJ}(\mathbf{1}) \epsilon^\nu(2) \ell_{A\alpha} \left(\eta^{\rho\alpha} - \frac{p^\rho p^\alpha}{M^2} \right) \\
 &= 2M^2 \left[(\epsilon(\mathbf{1}) \cdot \epsilon(2))(p_1 - p_2) \cdot \ell_A - 2 \left(\ell_A \cdot \epsilon(\mathbf{1}) p_1 \cdot \epsilon(2) - \ell_A \cdot \epsilon(2) p_2 \cdot \epsilon(\mathbf{1}) \right) \right] + M^4 \epsilon(\mathbf{1}) \cdot \epsilon(2)
 \end{aligned}
 \tag{22}$$

where $2\ell_A \cdot \mathbf{p} = M^2$. We also have a contact term:

$$\text{Contact-Term} [\mathbf{1}, \mathbf{2}] = \epsilon(\mathbf{1}) \cdot \epsilon(2).
 \tag{23}$$

Collecting our results, and restoring color factors and the factor g/M^2 in the t -channel, we have:

$$\begin{aligned}
 A_4(\ell_{iA}, \mathbf{1}^a, \mathbf{2}^b, \ell_{jB}) &= 2\sqrt{2} g^2 T_{ik}^a T_{kj}^b \frac{\langle \mathbf{1}|\ell_A|\mathbf{1} \rangle}{M} \frac{\ell_B^\mu \epsilon_\mu(2)}{(\ell_A + \mathbf{1})^2 - m^2} + 2\sqrt{2} g^2 T_{ik}^b T_{kj}^a \frac{\langle \mathbf{1}|\ell_B|\mathbf{1} \rangle}{M} \frac{\ell_A^\mu \epsilon_\mu(2)}{(\ell_B + \mathbf{1})^2 - m^2} \\
 &- if^{abc} T_{ij}^c g^2 \left\{ 2 \left[(\epsilon(\mathbf{1}) \cdot \epsilon(2))(p_1 - p_2) \cdot \ell_A - 2 \left(\ell_A \cdot \epsilon(\mathbf{1}) p_1 \cdot \epsilon(2) - \ell_A \cdot \epsilon(2) p_2 \cdot \epsilon(\mathbf{1}) \right) \right] + M^2 \epsilon(\mathbf{1}) \cdot \epsilon(2) \right\} \\
 &\times \frac{1}{(p_1 + p_2)^2 - M^2} \\
 &+ g^2 \{T^a, T^b\}_{ij} \epsilon(\mathbf{1}) \cdot \epsilon(2).
 \end{aligned}
 \tag{24}$$

Observe that swapping the labels “gluon” and “Merlin” results in a change in the sign of the last term in the t -channel:

$$\begin{aligned}
 A_4(\ell_{iA}, \mathbf{1}^a, \mathbf{2}^b, \ell_{jB}) &= 2\sqrt{2}g^2 T_{ik}^a T_{kj}^b \frac{\langle \mathbf{2} | \ell_B | \mathbf{2} \rangle}{M} \ell_A^\mu \epsilon_\mu(1) \frac{1}{(\ell_B + \mathbf{2})^2 - m^2} \\
 &+ 2\sqrt{2}g^2 T_{ik}^b T_{kj}^a \frac{\langle \mathbf{2} | \ell_A | \mathbf{2} \rangle}{M} \ell_B^\mu \epsilon_\mu(1) \frac{1}{(\ell_A + \mathbf{2})^2 - m^2} \\
 &- if^{abc} T_{ij}^c g^2 \left\{ 2 \left[(\epsilon(1) \cdot \epsilon(2))(p_1 - p_2) \cdot \ell_A - 2 \left(\ell_A \cdot \epsilon(1) p_1 \cdot \epsilon(2) - \ell_A \cdot \epsilon(2) p_2 \cdot \epsilon(1) \right) \right] - M^2 \epsilon(1) \cdot \epsilon(2) \right\} \\
 &\times \frac{1}{(p_1 + p_2)^2 - M^2} \\
 &+ g^2 \{ T^b, T^a \}_{ij} \epsilon(1) \cdot \epsilon(2).
 \end{aligned} \tag{25}$$

Let us verify whether the above amplitude satisfies color–kinematics duality. We write:

$$A_4(\ell_{iA}, \mathbf{1}^a, \mathbf{2}^b, \ell_{jB}) = \frac{c_s n_s}{(\ell_A + p_1)^2 - m^2} + \frac{c_u n_u}{(\ell_A + p_2)^2 - m^2} - \frac{c_t n_t}{(p_1 + p_2)^2 - M^2} \tag{26}$$

where we have defined the following numerators

$$\begin{aligned}
 n_s &= 2\sqrt{2}g^2 \frac{\langle \mathbf{1} | \ell_A | \mathbf{1} \rangle}{M} \ell_B^\mu \epsilon_\mu(2) + g^2 \epsilon(\mathbf{1}) \cdot \epsilon(2) (2\ell_A \cdot p_1 + M^2) \\
 n_u &= 2\sqrt{2}g^2 \frac{\langle \mathbf{1} | \ell_B | \mathbf{1} \rangle}{M} \ell_A^\mu \epsilon_\mu(2) + g^2 \epsilon(\mathbf{1}) \cdot \epsilon(2) (2\ell_A \cdot p_2) \\
 n_t &= g^2 \left\{ 2 \left[(\epsilon(\mathbf{1}) \cdot \epsilon(2))(p_1 - p_2) \cdot \ell_A - 2 \left(\ell_A \cdot \epsilon(\mathbf{1}) p_1 \cdot \epsilon(2) - \ell_A \cdot \epsilon(2) p_2 \cdot \epsilon(\mathbf{1}) \right) \right] + M^2 \epsilon(\mathbf{1}) \cdot \epsilon(2) \right\}
 \end{aligned} \tag{27}$$

and color factors

$$\begin{aligned}
 c_s &= T_{ik}^a T_{kj}^b \\
 c_u &= T_{ik}^b T_{kj}^a \\
 c_t &= if^{abc} T_{ij}^c = [T^a, T^b]_{ij}.
 \end{aligned} \tag{28}$$

Observe that c_t is antisymmetric under an interchange of two legs, and the corresponding numerator n_t also obeys this property (to see this for the last term, one must check the construction of the amplitude given above). Moreover, $c_s - c_u = c_t$ implies that $n_s - n_u = n_t$. Thus, we have obtained a representation for the amplitude that satisfies the color–kinematics duality. A similar result is obtained for the other amplitude; that is,

$$A_4(\ell_{iA}, \mathbf{1}^a, \mathbf{2}^b, \ell_{jB}) = \frac{c_s n_s}{(\ell_A + p_2)^2 - m^2} + \frac{c_u n_u}{(\ell_A + p_1)^2 - m^2} - \frac{c_t n_t}{(p_1 + p_2)^2 - M^2} \tag{29}$$

with

$$\begin{aligned}
 n_s &= 2\sqrt{2}g^2 \frac{\langle \mathbf{2} | \ell_B | \mathbf{2} \rangle}{M} \ell_A^\mu \epsilon_\mu(1) + g^2 \epsilon(1) \cdot \epsilon(2) (2\ell_A \cdot p_1) \\
 n_u &= 2\sqrt{2}g^2 \frac{\langle \mathbf{2} | \ell_A | \mathbf{2} \rangle}{M} \ell_B^\mu \epsilon_\mu(1) + g^2 \epsilon(1) \cdot \epsilon(2) (2\ell_A \cdot p_2 + M^2) \\
 n_t &= g^2 \left\{ 2 \left[(\epsilon(1) \cdot \epsilon(2))(p_1 - p_2) \cdot \ell_A - 2 \left(\ell_A \cdot \epsilon(1) p_1 \cdot \epsilon(2) - \ell_A \cdot \epsilon(2) p_2 \cdot \epsilon(1) \right) \right] - M^2 \epsilon(1) \cdot \epsilon(2) \right\}
 \end{aligned} \tag{30}$$

and

$$\begin{aligned}
 c_s &= T_{ik}^a T_{kj}^b \\
 c_u &= T_{ik}^b T_{kj}^a \\
 c_t &= if^{abc} T_{ij}^c = [T^a, T^b]_{ij}.
 \end{aligned} \tag{31}$$

3. Brief Review of the Double-Copy Method and Gravity Amplitudes

As a consequence of the color–kinematics duality, one can derive amplitudes for a gravity theory with a spectrum which is the square of the Yang–Mills spectrum. One only needs to substitute color factors for kinematic factors in the corresponding gauge-theory amplitude [124–136]:

$$M_n = \sum_k \frac{n_k n_k}{s_k}. \tag{32}$$

We suppressed a factor of the coupling $(\kappa/2)^{n-2}$ at n points, where $\kappa^2 = 32\pi G$. This is the BCJ double-copy relation. The squaring relation can be generalized to

$$M_n = \sum_k \frac{\tilde{n}_k n_k}{s_k} \tag{33}$$

where \tilde{n}_k and n_k belong to two distinct Yang–Mills numerators, with only one of them constrained to satisfy the color–kinematics duality.

One can also use the color–kinematics relation together with the BCJ relations to rewrite gravity amplitudes as products of partial Yang–Mills amplitudes. The set of relations obtained in this way are called Kawai–Lewellen–Tye (KLT) relations [137]. The KLT relation streamlines the usual cumbersome calculations found when dealing with gravitational interactions: gravity tree amplitudes can be written in terms of gauge-theory partial amplitudes. Through four points, these relations are given by

$$\begin{aligned} M_3^{\text{tree}}(1, 2, 3) &= iA_3^{\text{tree}}[1, 2, 3]A_3^{\text{tree}}[1, 2, 3] \\ M_4^{\text{tree}}(1, 2, 3, 4) &= -is_{12}A_4^{\text{tree}}[1, 2, 3, 4]A_4^{\text{tree}}[1, 2, 4, 3] \end{aligned} \tag{34}$$

where M_n^{tree} are tree-level gravity amplitudes. The basic building block is given by gauge-theory tree-level scattering amplitudes.

The KLT relations are usually constructed for massless amplitudes, but a double-copy prescription for Weyl gravity was put forward in [84,85,87]. Similar to the gauge-theory case, we also verify an unusual feature: Since standard BCJ relations are not obeyed by four-point gauge amplitudes, the corresponding KLT relations are not satisfied by four-point quadratic-gravity amplitudes. This feature was duly explored in [87] in order to build up a consistent map to relate gauge amplitudes with gravity amplitude through a double-copy prescription. This map is given by

$$(\text{Higher-derivative YM}) \otimes \text{YM} = \text{Weyl-Einstein} \tag{35}$$

which was motivated by the considerations studied in [84,85]. The action that describes the Weyl–Einstein theory reads

$$S = \int d^4x \sqrt{-g} \left[\frac{2}{\kappa^2} R - \frac{1}{2\xi^2} C_{\mu\nu\alpha\beta} C^{\mu\nu\alpha\beta} \right] \tag{36}$$

where $C_{\mu\nu\alpha\beta}$ is the Weyl tensor. This action also describes the more general quadratic-gravity theory in the Einstein frame. This can be obtained through a simple field redefinition from the Jordan-frame action [138]:

$$S = \int d^4x \sqrt{-g} \left[\frac{2}{\kappa^2} R + \frac{1}{6f_0^2} R^2 - \frac{1}{2\xi^2} C_{\mu\nu\alpha\beta} C^{\mu\nu\alpha\beta} \right]. \tag{37}$$

Essentially the difference between the two frames is that in the former we verify the presence of an extra scalar field with a particular interaction potential whose contribution is usually added to the matter sector.

As extensively discussed in [87], the map given by Equation (35) does not yield a pure Weyl–Einstein gravity. Typically, the double copy of two vector fields produces gravitons, a

dilaton and an axion. For quadratic gravity, the map Equation (35) produces, besides such degrees of freedom, the associated Merlins with each of those particles. The projection to pure gravity can be obtained by correlating the helicities in the two gauge-theory copies (for the graviton) and by taking the symmetric tensor product of gauge-theory Merlins (for the gravitational Merlin). On the other hand, the map (35) requires, for consistency, the consideration of spontaneously broken gauge theories. In other words, the pure YM part of the double copy must comprise massive gauge fields. For a thorough discussion, we refer the reader to [87]. For an interesting account of the double-copy construction for spontaneously broken gauge theories, see [139–141].

The polarization tensors of massive Merlin particles can be constructed as tensor products of the spin-1 polarization vectors [57]:

$$[\epsilon^{\alpha\dot{\alpha}}]^{(S)} = [\epsilon^{\alpha\dot{\alpha}}]^{\otimes S} = \left(\frac{\sqrt{2}}{M}\right)^S (|\mathbf{p}\rangle[\mathbf{p}])^S \tag{38}$$

where symmetrization in the spinor products is implicitly understood.

Let us now list the on-shell amplitudes that will enter in the forthcoming calculations. As above, we begin with three-point amplitudes. Three-particle amplitudes involving only physical gravitons do not display contributions coming from higher-order derivative terms [85,87,142],

$$M_3^{(4)}[1^{h_1}, 2^{h_2}, 3^{h_3}] = M^2 M_3^{(2)}[1^{h_1}, 2^{h_2}, 3^{h_3}] \tag{39}$$

(h_i represents a given graviton helicity) where

$$\begin{aligned} M_3^{(2)}(1^-, 2^-, 3^+) &= \left(A_3^{(2)}[1^-, 2^-, 3^+]\right)^2 = \frac{\langle 12 \rangle^6}{\langle 13 \rangle^2 \langle 32 \rangle^2} \\ M_3^{(2)}[1^+, 2^+, 3^-] &= \left(A_3^{(2)}[1^+, 2^+, 3^-]\right)^2 = \frac{[12]^6}{[13]^2 [32]^2}. \end{aligned} \tag{40}$$

This result generalizes to an arbitrary number of gravitons by employing BCFW recursion relations. In turn, amplitudes with a single gravitational Merlin particle vanish [85,87]:

$$M_{n+1}^{(4)}(1^{h_1}, 2^{h_2}, \dots, n^{h_n}, \mathbf{k}) = 0 \tag{41}$$

The three-particle amplitude involving two gravitational Merlin particles and one graviton may be obtained from the YM case by using the KLT relations discussed in [121]:

$$\begin{aligned} M_3(1^{++}, \mathbf{2}, \mathbf{3}) &= iA_3^{\text{tree,HD}}[1^+, \mathbf{2}, \mathbf{3}]A_3^{\text{tree,YM}}[1^+, \mathbf{2}, \mathbf{3}] = -2i \frac{\langle r|\mathbf{3}|1\rangle^2}{M^4 \langle r1 \rangle^2} \langle \mathbf{32} \rangle^4 \\ M_3(1^{--}, \mathbf{2}, \mathbf{3}) &= iA_3^{\text{tree,HD}}[1^-, \mathbf{2}, \mathbf{3}]A_3^{\text{tree,YM}}[1^-, \mathbf{2}, \mathbf{3}] = -2i \frac{[r|\mathbf{3}|1]^2}{M^4 [1r]^2} [\mathbf{32}]^4. \end{aligned} \tag{42}$$

To complete our list of required three-particle amplitudes, we need the ones involving one gravitational particle (graviton or Merlin) and two massive scalars. The double-copy prescription was given in [121]. The graviton case reads

$$\begin{aligned} M_3^{\text{tree}}(\ell_A^+, p^{++}, \ell_B^-) &= i\left(A_3^{\text{tree,YM}}[\ell_A^+, p^+, \ell_B^-]\right)^2 \\ &= 2i \frac{\langle \xi | \ell_A | p \rangle^2}{\langle \xi p \rangle^2} \end{aligned} \tag{43}$$

whereas in the Merlin case the amplitude is given by [87]

$$\begin{aligned} M_3^{\text{tree}}(\ell_A^+, \mathbf{p}, \ell_B^-) &= iA_3^{\text{tree,HD}}[\ell_A^+, \mathbf{p}, \ell_B^-]A_3^{\text{tree,YM}}[\ell_A^+, \mathbf{p}, \ell_B^-] \\ &= 2i \frac{\langle \mathbf{p} | \ell_A | \mathbf{p} \rangle^2}{M^2}. \end{aligned} \tag{44}$$

Let us now display the four-point amplitudes that go into the formulas of the leading singularities below. Amplitudes involving only gravitons can be obtained from the usual KLT relations. Likewise, amplitudes with gravitational Merlin particles and gravitons can also be derived with the same procedure [87]. For instance, the amplitude $M_4[1^{++}, 2, 3, 4^{++}]$, which involves two gravitational Merlin particles, reads [87,121]

$$M_4^{\text{tree}}(2, 1^{++}, 4^{++}, 3) = -is_{23}A_4^{\text{tree, HD}}[2, 1^+, 4^+, 3]A_4^{\text{tree, YM}}[2, 4^+, 1^+, 3] = 4i \frac{[14]^4}{s_{23}} \frac{\langle 32 \rangle^4}{(s_{12} - M^2)(s_{13} - M^2)}. \tag{45}$$

where $s_{ij} = (p_i + p_j)^2$. As for the amplitudes involving scalar matter particles, we find that [119,121]

$$\begin{aligned} M_4(1, 2^{++}, 3^{--}, 4) &= -i \frac{\langle 3|1|2 \rangle^4}{[(p_1 + p_2)^2 - m^2][(p_1 + p_3)^2 - m^2](p_2 + p_3)^2} \\ M_4(1, 2^{--}, 3^{--}, 4) &= -im^4 \frac{\langle 23 \rangle^4}{(p_2 + p_3)^2 [(p_1 + p_2)^2 - m^2][(p_1 + p_3)^2 - m^2]} \end{aligned} \tag{46}$$

for gravitons (reverse helicity amplitudes can be obtained from the above formulas by swapping angle and square brackets) and

$$\begin{aligned} M_4(\ell_A, 1, 2, \ell_B) &= \left[\frac{2}{M^2} \langle 1|\ell_A|1 \rangle \langle 2|\ell_B|2 \rangle + \frac{\langle 12 \rangle [21]}{M^2} (2(1 \cdot \ell_A) + M^2) \right]^2 \frac{i}{(\ell_A + p_1)^2 - m^2} \\ &+ \left[\frac{2}{M^2} \langle 1|\ell_B|1 \rangle \langle 2|\ell_A|2 \rangle + \frac{\langle 12 \rangle [21]}{M^2} (2(2 \cdot \ell_A) + M^2) \right]^2 \frac{i}{(\ell_A + p_2)^2 - m^2} \\ &- \frac{4i}{M^4} \left(\langle 12 \rangle [21] (1 - 2) \cdot \ell_A + \langle 1|\ell_A|1 \rangle \langle 2|\ell_B|2 \rangle - \langle 2|\ell_A|2 \rangle \langle 1|\ell_B|1 \rangle \right)^2 \left(\frac{1}{(p_1 + p_2)^2} - \frac{2}{(p_1 + p_2)^2 - M^2} \right). \end{aligned} \tag{47}$$

for Merlins [87]. The former can be derived from the double-copy formula

$$M^{\text{tree}}(1_s, 2, 3, 4_s) = i \left(\frac{\kappa}{2} \right)^2 s_{23} (-1)^{[s] - [s_1] - [s_2] + 1} A^{\text{tree}}[1_{s_1}, 2, 3, 4_{s_1}] A^{\text{tree}}[1_{s_2}, 3, 2, 4_{s_2}], \quad s = s_1 + s_2 \tag{48}$$

as proposed in [121]. The amplitude with Merlins can be derived from the relation [87]

$$M(1_s, 2, 3, 4_s) = i \sum_k \frac{n_k^{(s_1)}(1_{s_1}, 2, 3, 4_{s_1}) \tilde{n}_k^{(s_2)}(1_{s_2}, 2, 3, 4_{s_2})}{s_k} \tag{49}$$

where $s = s_1 + s_2$, s_1, s_2 are the associated spins of the matter particles, 2, 3 are graviton or Merlin particles, \tilde{n}_k are numerators from the spontaneously broken gauge theory of the double copy and s_k are inverse propagators. The double-copy relation (49) implies that Equation (47) necessarily contains all the degrees of freedom produced by the double copy in the t -channel. In order to allow for only gravitons and gravitational Merlins to flow through the cuts of the t -channel, one may employ four-dimensional physical state projectors, defined as

$$\begin{aligned} \sum_{\lambda=\pm 2} \epsilon_{\lambda}^{\mu\nu}(p; r) \epsilon_{\lambda}^{\rho\sigma*}(p; r) &= \frac{1}{2} \left(\pi_{\mu\rho} \pi_{\nu\sigma} + \pi_{\mu\sigma} \pi_{\nu\rho} - \pi_{\mu\nu} \pi_{\rho\sigma} \right) \quad (\text{Graviton}) \\ \pi_{\mu\nu} &= \eta_{\mu\nu} - \frac{p_{\mu} \bar{p}_{\nu} + p_{\nu} \bar{p}_{\mu}}{p \cdot \bar{p}} \\ \sum_{\lambda=-2} \epsilon_{\lambda}^{\mu\nu} \epsilon_{\lambda}^{\rho\sigma*} &= \frac{1}{2} \left(\tilde{\pi}_{\mu\rho} \tilde{\pi}_{\nu\sigma} + \tilde{\pi}_{\mu\sigma} \tilde{\pi}_{\nu\rho} - \frac{2}{3} \tilde{\pi}_{\mu\nu} \tilde{\pi}_{\rho\sigma} \right) \quad (\text{Merlin}) \\ \tilde{\pi}_{\mu\nu} &= \eta_{\mu\nu} - \frac{p_{\mu} p_{\nu}}{M^2}. \end{aligned} \tag{50}$$

where $\bar{p}^{\mu} = (p^0, -\mathbf{p})$.

As in the previous case, our computations will require a four-point amplitude with a Merlin and a graviton as external states. Since the associated gauge-theory amplitude obeys color-kinematics duality, the evaluation of the corresponding gravity amplitude goes through the use of the double-copy prescription as given by Equation (49). We obtain

$$\begin{aligned}
 &M_4(\ell_A, \mathbf{1}, 2, \ell_B) \\
 &= \left[2\sqrt{2} \frac{\langle \mathbf{1} | \ell_A | \mathbf{1} \rangle}{M} \ell_B^\mu \epsilon_\mu(2) + \epsilon(1) \cdot \epsilon(2) (2\ell_A \cdot p_1 + M^2) \right]^2 \frac{i}{(\ell_A + p_1)^2 - m^2} \\
 &+ \left[2\sqrt{2} \frac{\langle \mathbf{1} | \ell_B | \mathbf{1} \rangle}{M} \ell_A^\mu \epsilon_\mu(2) + g^2 \epsilon(1) \cdot \epsilon(2) (2\ell_A \cdot p_2) \right]^2 \frac{i}{(\ell_A + p_2)^2 - m^2} \\
 &+ \left\{ 2 \left[(\epsilon(1) \cdot \epsilon(2)) (p_1 - p_2) \cdot \ell_A - 2(\ell_A \cdot \epsilon(1) p_1 \cdot \epsilon(2) - \ell_A \cdot \epsilon(2) p_2 \cdot \epsilon(1)) \right] + M^2 \epsilon(1) \cdot \epsilon(2) \right\}^2 \frac{i}{(p_1 + p_2)^2 - M^2} \quad (51)
 \end{aligned}$$

and also

$$\begin{aligned}
 &M_4(\ell_A, \mathbf{1}, 2, \ell_B) \\
 &= \left[2\sqrt{2} \frac{\langle \mathbf{2} | \ell_A | \mathbf{2} \rangle}{M} \ell_B^\mu \epsilon_\mu(1) + \epsilon(1) \cdot \epsilon(2) (2\ell_A \cdot p_2 + M^2) \right]^2 \frac{i}{(\ell_A + p_2)^2 - m^2} \\
 &+ \left[2\sqrt{2} \frac{\langle \mathbf{2} | \ell_B | \mathbf{2} \rangle}{M} \ell_A^\mu \epsilon_\mu(1) + \epsilon(1) \cdot \epsilon(2) (2\ell_A \cdot p_1) \right]^2 \frac{i}{(\ell_A + p_1)^2 - m^2} \\
 &+ \left\{ 2 \left[(\epsilon(1) \cdot \epsilon(2)) (p_1 - p_2) \cdot \ell_A - 2(\ell_A \cdot \epsilon(1) p_1 \cdot \epsilon(2) - \ell_A \cdot \epsilon(2) p_2 \cdot \epsilon(1)) \right] - M^2 \epsilon(1) \cdot \epsilon(2) \right\}^2 \frac{i}{(p_1 + p_2)^2 - M^2}. \quad (52)
 \end{aligned}$$

The overall minus sign in the t -channel comes from the difference in signs of the associated numerators coming from the two different gauge theories in the double-copy map. Furthermore, similar to Equation (47), both expressions comprise all the Merlin degrees of freedom produced by the double copy flowing in the t -channel.

4. Leading Singularities in One-Loop Processes Involving Merlin Particles

We are now in the position to calculate the leading singularities of one-loop amplitudes. As discussed above, we are interested in gluon as well as graviton scatterings in the corresponding higher-derivative theories. Moreover, we are also going to consider the one-loop four-point scattering process of massive scalars proceeding via the exchange of gauge as well as gravitational particles. We will consider the narrow-width approximation for the associated Merlin propagators. We are going to consider two different topologies for the leading singularities, that is, box and triangle. These are depicted in Figure 1.

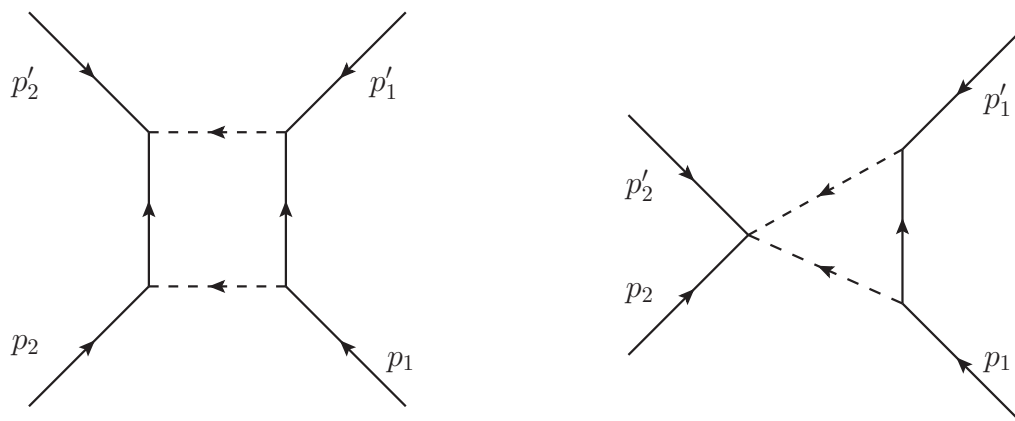


Figure 1. Different topologies for the calculation of the leading singularities. Thick lines represent all possible external particles considered in the text, whereas dashed lines represent intermediate states.

Let us briefly outline the necessary steps to implement the technique before moving on to the actual calculation. As discussed above, generalized unitarity explores discontinuities in loop diagrams. The important point is that, as in the case of standard unitarity cuts associated with two-particle exchanges, the additional cuts can also be realized as contour integrals. That this is a mandatory treatment for leading singularities can be noticed from the fact that unitarity methods require the replacement of propagators by on-shell delta functions—for more than two massless propagators, the solutions to the on-shell equations are complex, and the associated delta functions can only yield zero. Thus, a well-defined procedure leads one to consider contour integrals instead of delta functions [23]. Every time a residue is evaluated, one uncovers a higher co-dimension singularity. The maximal number of residues at the L -loop order is $4L$ in four dimensions. Evaluating all $4L$ residues generates the highest co-dimension singularity—the corresponding discontinuity is the leading singularity [54,55].

As mentioned above, the support of the delta functions is outside the physical region where the loop momentum is a real vector. This suggests that the integration procedure associated with the leading singularity should be carried out in terms of contour integrals in \mathbb{C}^4 , and the loop momentum is therefore to be regarded as a complex vector. By applying the four-dimensional loop-momentum integral over each such contour, one obtains the residue at the associated encircled pole. Contrary to the product of delta functions, the transformations here yield a factor of the inverse of the Jacobian. This ensures that we obtain an analytic result, and hence further contour integrations can be carried out [54,55]. As we will see in the course of the calculations, in our case there will be two distinct leading singularities.

As discussed in [69], unitarity-based methods are still useful in theories containing resonances; one only needs to verify whether the external momentum configurations of the amplitude allow the unstable propagator to become resonant. When one is off resonance, one possible way to deal with unstable particles is to eliminate them through the use of a description which contains only stable modes, albeit a non-local one [69]. When the coupling to the decay products is very small, and therefore only resonance production is important, one may resort to the narrow-width approximation in order to circumvent such issues.

On the other hand, in theories containing Merlin modes, close to the resonance the Merlin propagator has the generic form

$$iD(q) \sim \frac{-i}{q^2 - m^2 - i\gamma}$$

where γ is associated with its decay width. As observed above, the presence of the two unusual minus signs is important for unitarity—this is a consequence of the fact that the imaginary part of the Merlin propagator is the same as that of a normal resonance, as can be seen from the expression above:

$$\text{Im}[D(q)] \sim \frac{-\gamma^2}{(q^2 - m^2)^2 + \gamma^2}.$$

Since we are interested in calculating contour integrals along adequate contours which are associated with the process of cutting propagators, which in turn yields the corresponding imaginary parts, two sets of amplitudes with different propagators which nevertheless have the same imaginary parts will generate identical results for the aforementioned contour integral. This means that the fact that leading singularities make sense in theories with unstable particles indicates that these are also available in the study of the analytic properties of loop amplitudes containing Merlin modes. This was precisely one of the key points raised in [69].

A slight difference arises here. First, observe that, for stable particles and normal unstable particles, the sign of the residue of the one-particle pole is opposite to that of

the imaginary part of that pole. For the Merlin particle such signs are equal—a similar result was also found in [143]. On the other hand, in the narrow-width approximation, the cut of a Merlin propagator should produce the same delta function as of a normal resonance. However, the Merlin propagator has an overall minus sign; when taking its propagator to define a variable $1/u$ and then integrate over a contour $|u| = \epsilon$ encircling $u = 0$ in the complex plane, the resulting residue has the opposite sign of the normal resonance. However, both operations should be equivalent. Such observations motivate us to define the contours for the leading singularities involving Merlins in such a way that their orientations should be the opposite to that of a normal resonance. This is necessary as positive energy flow associated with the Merlin propagates backward in time; furthermore, the residue at the Merlin pole is always negative and the sign of the width is always opposite from normal resonances. A related modification was put forward in [59] when discussing unitarity in the framework of Veltman’s largest time equation.

In a sense, the fact that amplitudes with ghost and normal resonances can be reconstructed by using unitarity-based methods can be seen as a non-trivial corollary of the results given in [59,64]. Indeed, from Veltman’s work it is known that normal resonances satisfy unitarity to all orders in perturbation theory. Thence any discontinuity computed considering normal resonances in the intermediate states can be translated to a discontinuity with ghost resonances by using the fact that such resonances can be described in the same propagator with the coupling to the stable states described by the same self-energy; that is,

$$iD(q) = \frac{i}{q^2 - m^2 + \Sigma(q) - q^4/\Lambda^2}.$$

Hence, it follows that, if the normal resonance satisfies the unitarity constraint, the ghost resonance must also. Therefore unitarity-based methods (including leading singularities) can be successfully applied to amplitudes involving all such resonances, as argued in [69].

4.1. Higher-Derivative Yang–Mills

4.1.1. Gluon Scattering

Here, we will study a specific one-loop gluon scattering $g^+g^+ \rightarrow g^+g^+$ proceeding in the higher-derivative Yang–Mills theory. The leading singularity formula with gluons running in the loop is given by

$$LS_g^{(g)} = \sum_{h_1, h_3, h=\pm} \oint_{\Gamma} \frac{d^4\ell}{(2\pi)^4} \frac{1}{\ell^2(\ell + p'_1)^2(\ell - p_1)^2} A_3[1'^+, \ell^{-h}, -\ell^{h_1}] A_3[-\ell^h, 1^+, -\ell^{h_3}] A_4[2^+, \ell_3^{-h_3}, \ell_1^{-h_1}, 2'^+] \quad (53)$$

where $\ell_1 = \ell + p'_1$ and $\ell_3 = p_1 - \ell$. For Merlins running in the loop, we find that

$$LS_M^{(g)} = \oint_{-\Gamma} \frac{d^4\ell}{(2\pi)^4} \frac{-1}{(\ell^2 - M^2)} \frac{-1}{[(\ell + p'_1)^2 - M^2]} \frac{-1}{[(\ell - p_1)^2 - M^2]} A_3[1'^+, \ell, -\ell_1] A_3[-\ell, 1^+, -\ell_3] A_4[2^+, \ell_3, \ell_1, 2'^+]. \quad (54)$$

In the above formulae, we take color-ordered amplitudes as the result, and the full amplitudes can be obtained in the same way as will now be described. Notice also that these are the only possible configurations due to the fact that amplitudes with only one Merlin vanish. Generically, the contour Γ is defined as enclosing all the corresponding poles produced by cutting the propagators—the minus in front of it in the expression for $LS_M^{(g)}$ is to remind us that the contour associated with a Merlin pole must have the opposite orientation to that corresponding to a stable particle (or a normal resonance).

We begin our discussion with the associated scattering with gluons running in the loop. First consider the triangle topology for the leading singularity. In principle, the only contribution in the sum over the helicities h_1, h_3 in $LS_{\Delta g}^{(g)}$ would be the term corresponding to $h_1 = h_3 = +$. However, a quick inspection of the remainder, that is,

$$LS_{\Delta g}^{(g)} = \sum_{h=\pm} \oint_{\Gamma} \frac{d^4\ell}{(2\pi)^4} \frac{1}{\ell^2(\ell + p'_1)^2(\ell - p_1)^2} A_3[1'^+, \ell^{-h}, -\ell_1^+] A_3[-\ell^h, 1^+, -\ell_3^+] A_4[2^+, \ell_3^-, \ell_1^-, 2'^+] \quad (55)$$

reveals that it is actually zero. Thus, in pure Yang–Mills theories, the triangle leading singularity associated with the one-loop scattering $A_4^{1\text{-loop}}[1'^+, 1^+, 2^+, 2'^+]$ vanishes. What about the box leading singularity? With a judicious choice of reference spinors for the three-point amplitudes, one can show that the associated product of three-point amplitudes vanishes. Thus, the box leading singularity is also zero.

The fact that both leading singularities are zero should not come as a surprise. One-loop gluon amplitudes with gluons running in the loops can be calculated from the following identity [19,37,38,122,144]:

$$A^{1\text{-loop}} = A^{\mathcal{N}=4} - 4A^{\mathcal{N}=1} + A^{\text{scalar}} \tag{56}$$

where $A^{\mathcal{N}=4}$ is the corresponding amplitude in the $\mathcal{N} = 4$ super Yang–Mills theory, $A^{\mathcal{N}=1}$ is the $\mathcal{N} = 1$ amplitude with a chiral multiplet in the loop and A^{scalar} is the non-supersymmetric amplitude with a complex scalar in the loop. Since all-plus gluon amplitude vanishes to all orders in perturbation theory for supersymmetric theories, $A^{1\text{-loop}}$ can be calculated by considering only complex scalars circulating in the loop—but this amplitude consists of purely rational terms, which are cut-free in four dimensions. A non-trivial result can only be obtained by going to $D = 4 - 2\epsilon$ dimensions. Hence, its leading singularity must be zero in four dimensions.

Now, let us study the case of Merlin particles running in the loop. We may proceed as in [55]—recall that the contour encircling a Merlin pole must have the opposite orientation as the one for a normal particle. We find that

$$\text{LS}_M^{(g)} = -\frac{1}{8(p_1 \cdot p'_1)} \frac{1}{(2\pi i)} \oint_{\Gamma} \frac{dz}{z} A_3[1'^+, \ell, -\ell_1] A_3[-\ell, 1^+, -\ell_3] A_4[2^+, \ell_3, \ell_1, 2'^+]. \tag{57}$$

The product of the amplitudes can be easily calculated:

$$A_3[1'^+, \ell, -\ell_1] A_3[-\ell, 1^+, -\ell_3] A_4[2^+, \ell_3, \ell_1, 2'^+] = -24M^{12} \frac{[22'] [11']}{\langle 22' \rangle \langle 11' \rangle} \frac{1}{(p_2 + \ell_3)^2 - M^2} \tag{58}$$

where we have factored out g/M^2 . Observe that this expression corrects the overall numeric factor found in an analogous formula in [87]. Using similar parameterizations as in [55], we find that

$$\text{LS}_M^{(g)} = M^{12} \frac{[11'] [22']}{\langle 11' \rangle \langle 22' \rangle} \frac{1}{(2\pi i)} \oint_{\Gamma} \frac{dz}{z} \frac{3z}{-2(p_1 \cdot p'_1)(\bar{q} \cdot p_2)z^2 + 2(p_1 \cdot p'_1)(p_1 \cdot p_2)z + M^2 q \cdot p_2}. \tag{59}$$

where $q^{\alpha\dot{\alpha}} = |1'\rangle [1]$ and the corresponding conjugate $\bar{q}^{\alpha\dot{\alpha}} = |1\rangle [1']$ are fixed reference massless vectors. We define the contour Γ associated with the triangle topology as the contour enclosing either of the poles at $z = \infty$ and $z = 0$. Choosing any of them will lead to $\text{LS}_{\Delta M}^{(g)} = 0$. On the other hand, circling one of the two solutions of the quadratic factor that arises in the denominator will lead to the box topology. We obtain

$$\text{LS}_{\square M}^{(g)} = -g^4 \frac{ut}{\langle 11' \rangle \langle 1'2 \rangle \langle 22' \rangle \langle 2'1 \rangle} \frac{6M^4}{\sqrt{s^2 u^2 + 4M^2 stu}} \tag{60}$$

where the Mandelstam variables are defined as usual; that is, $s = (p_1 + p_2)^2$, $t = (p_1 + p'_2)^2$ and $u = (p_1 + p'_1)^2$, with $s + t + u = 0$. We also restored the g/M^2 factors. Thus, we see that the leading singularity associated with the one-loop scattering amplitude $A_4^{1\text{-loop}}[1'^+, 1^+, 2^+, 2'^+]$ does not vanish in the higher-derivative Yang–Mills theory. This is a consequence of the presence of massive Merlin modes running in the loops. Moreover, only the box topology is non-trivial—essentially this is due to the fact that in the expression of the one-loop amplitude only the box integral is present [87].

4.1.2. Scalar Scattering

Now, we wish to explore general leading singularities in the scattering of matter particles $\phi\phi \rightarrow \phi\phi$ via gluon and Merlin exchange. For simplicity, we will work with identical massive scalars. The associated expressions are given by

$$LS_g^{(s)} = \sum_{h_1, h_3} \oint_{\Gamma} \frac{d^4\ell}{(2\pi)^4(\ell^2 - m^2)} \frac{1}{(\ell + p'_1)^2(\ell - p_1)^2} A_3(\mathbf{1}'_j, \ell, -\ell^{h_1}) A_3(-\ell, \mathbf{1}_i, -\ell^{h_3}) A_4(\mathbf{2}_m, \ell_3^{-h_3}, \ell_1^{-h_1}, \mathbf{2}'_n) \quad (61)$$

for gluons running in the loop, whereas for Merlins we find that

$$LS_M^{(s)} = \oint_{-\Gamma} \frac{d^4\ell}{(2\pi)^4(\ell^2 - m^2)} \frac{-1}{[(\ell + p'_1)^2 - M^2]} \frac{-1}{[(\ell - p_1)^2 - M^2]} A_3(\mathbf{1}'_j, \ell, -\ell_1) A_3(-\ell, \mathbf{1}_i, -\ell_3) A_4(\mathbf{2}_m, \ell_3, \ell_1, \mathbf{2}'_n). \quad (62)$$

where m is the mass of the scalar particles. One also has two crossed terms:

$$LS_{gM}^{(s)} = \sum_{h=\pm} \oint_{-\Gamma} \frac{d^4\ell}{(2\pi)^4(\ell^2 - m^2)} \frac{1}{(\ell + p'_1)^2} \frac{-1}{[(\ell - p_1)^2 - M^2]} A_3(\mathbf{1}'_j, \ell, -\ell_1^h) A_3(-\ell, \mathbf{1}_i, -\ell_3) A_4(\mathbf{2}_m, \ell_3, \ell_1^{-h}, \mathbf{2}'_n)$$

$$LS_{Mg}^{(s)} = \sum_{h=\pm} \oint_{-\Gamma} \frac{d^4\ell}{(2\pi)^4(\ell^2 - m^2)} \frac{-1}{[(\ell + p'_1)^2 - M^2]} \frac{1}{(\ell - p_1)^2} A_3(\mathbf{1}'_j, \ell, -\ell_1) A_3(-\ell, \mathbf{1}_i, -\ell_3^h) A_4(\mathbf{2}_m, \ell_3^{-h}, \ell_1, \mathbf{2}'_n) \quad (63)$$

which contain a four-point amplitude with external Merlin and gluon, in addition to the scalars. There are actually other contributions that can be obtained from those above by considering $1 \leftrightarrow 2$. Thus, the calculation of those above will suffice to our purposes.

We begin with $LS_g^{(s)}$. The technique is similar to the one used in [55]. In the present case it will be instructive to describe it with some detail. We parametrize ℓ as

$$\ell = zL + \omega q \quad (64)$$

where $L^{\alpha\dot{\alpha}} = |L\rangle [L|$ and q is a fixed reference massless momentum. Now, the integration variables are $z, \omega \in \mathbb{C}$ and the helicity spinors $|L\rangle, |L|$. The measure becomes

$$\frac{d^4\ell}{\ell^2 - m^2} = zdz \langle LdL \rangle [LdL] \frac{d\omega}{4[\omega - m^2 / (2zL \cdot q)]}. \quad (65)$$

Contour integration around the pole $\ell^2 = m^2$ fixes $\omega = m^2 / (2zL \cdot q)$:

$$LS_g^{(s)} = \sum_{h_1, h_3} \frac{1}{4(2\pi i)^3} \oint_{\Gamma} \frac{zdz \langle LdL \rangle [LdL]}{(2m^2 + 2\ell \cdot p'_1)(2m^2 - 2\ell \cdot p_1)} A_3(\mathbf{1}'_j, \ell, -\ell^{h_1}) A_3(-\ell, \mathbf{1}_i, -\ell^{h_3}) A_4(\mathbf{2}_m, \ell_3^{-h_3}, \ell_1^{-h_1}, \mathbf{2}'_n). \quad (66)$$

Now, define two auxiliary massless vectors p_3, p_4 through the following relations:

$$p'_1 = p_3 + x_1 p_4$$

$$p_1 = p_4 + x_1 p_3$$

$$x_1 = \frac{m^2}{2p_3 \cdot p_4}. \quad (67)$$

From such definitions, one can show that

$$\frac{(1 + x_1)^2}{x_1} = \frac{(p_1 + p'_1)^2}{m^2}$$

$$\frac{(1 - x_1)^2}{x_1} = \frac{(p_1 + p'_1)^2 - 4m^2}{m^2}. \quad (68)$$

The reference massless vector q and its conjugate \bar{q} will be taken to be

$$q^{\alpha\dot{\alpha}} = |3\rangle [4|$$

$$\bar{q}^{\alpha\dot{\alpha}} = |4\rangle [3|. \quad (69)$$

Now, use the expansion

$$L = Ap_3 + Bp_4 + Cq + D\bar{q}. \tag{70}$$

We choose $D = 1$ as the overall scale of L is immaterial, and we find that $C = AB$ as a consequence of $L^2 = 0$. One finds that

$$L^{\alpha\dot{\alpha}} = |L\rangle [L] = (A|3\rangle + |4\rangle) ([3] + B[4]). \tag{71}$$

Therefore, with a simple change in the variables, one obtains that

$$LS_g^{(s)} = \frac{x_1}{4m^2} \frac{1}{(2\pi i)^3} \sum_{h_1, h_3} \oint_{\Gamma} \frac{zdz dAdB}{(2x_1 + z(Ax_1 + B))(2x_1 - z(A + Bx_1))} A_3(\mathbf{1}'_j, \ell, -\ell^{h_1}) A_3(-\ell, \mathbf{1}_i, -\ell^{h_3}) A_4(\mathbf{2}_m, \ell_3^{-h_3}, \ell_1^{-h_1}, \mathbf{2}'_n). \tag{72}$$

Contour integrations over the two visible poles fix

$$A = -B = \frac{2x_1}{z(1 - x_1)}$$

which leads us to

$$LS_g^{(s)} = \frac{x_1}{4m^2(1 - x_1^2)} \sum_{h_1, h_3} \frac{1}{(2\pi i)} \oint_{\Gamma} \frac{dz}{z} A_3(\mathbf{1}'_j, \ell, -\ell^{h_1}) A_3(-\ell, \mathbf{1}_i, -\ell^{h_3}) A_4(\mathbf{2}_m, \ell_3^{-h_3}, \ell_1^{-h_1}, \mathbf{2}'_n). \tag{73}$$

Now, let us explicitly evaluate the case with opposite helicities. Using the following parameterizations

$$\begin{aligned} \ell_1^{\alpha\dot{\alpha}}(z) &= |\ell_1\rangle [\ell_1] = r(x_1) \left(|3\rangle + \frac{z}{r(x_1)} |4\rangle \right) \left([3] - \frac{x_1}{z} r(x_1) [4] \right) \\ \ell_3^{\alpha\dot{\alpha}}(z) &= |\ell_3\rangle [\ell_3] = r(x_1) \left(|4\rangle + \frac{x_1}{z} r(x_1) |3\rangle \right) \left([4] - \frac{z}{r(x_1)} [3] \right) \\ r(x) &= \frac{1+x}{1-x} \end{aligned} \tag{74}$$

and the three-point amplitudes given above, one can prove that

$$LS_g^{(s+-)} = -\frac{g^2}{2} \frac{x_1^2}{(1 - x_1^2)} \left(\frac{1+x_1}{1-x_1} \right)^2 T_{jk}^c T_{ki}^d \frac{1}{2\pi i} \oint_{\Gamma} \frac{dz}{z^3} A_4(\mathbf{2}_m, \ell_3^{d+}, \ell_1^{c-}, \mathbf{2}'_n) \tag{75}$$

and

$$LS_g^{(s-+)} = -\frac{g^2}{2} \frac{1}{(1 - x_1^2)r(x_1)^2} T_{jk}^c T_{ki}^d \frac{1}{2\pi i} \oint_{\Gamma} dz z A_4(\mathbf{2}_m, \ell_3^{d-}, \ell_1^{c+}, \mathbf{2}'_n), \tag{76}$$

where the associated color factors coming from the three-point amplitudes are manifest. Let us focus on $LS_g^{(s+-)}$. For the purpose of calculating the leading singularity associated with the triangle topology with opposite helicities, it is useful to rewrite the Compton amplitude as

$$\begin{aligned} A_4(\mathbf{2}_m, \ell_3^{d+}, \ell_1^{c-}, \mathbf{2}'_n) &= -\frac{2g^2}{t} \left(\frac{T_{ml}^c T_{ln}^d}{2p_2 \cdot \ell_1} + \frac{T_{ml}^d T_{ln}^c}{2p'_2 \cdot \ell_1} \right) \langle \ell_1 | \mathbf{2} | \ell_3 \rangle^2 \\ &= -\frac{g^2}{t} \left(\frac{\{T^c, T^d\}_{mn} + [T^c, T^d]_{mn}}{2p_2 \cdot \ell_1} + \frac{\{T^d, T^c\}_{mn} + [T^d, T^c]_{mn}}{2p'_2 \cdot \ell_1} \right) \langle \ell_1 | \mathbf{2} | \ell_3 \rangle^2 \\ &= g^2 \{T^c, T^d\}_{mn} z^2 \frac{(z^2/r(x_1))^2 \bar{k} \cdot p_2 + z/r(x_1)(p_3 - p_4) \cdot p_2 - k \cdot p_2)^2}{[(\bar{k} \cdot p_2)/r(x_1)z^2 + (p_3 - x_1 p_4) \cdot p_2 z - x_1 r(x_1) k \cdot p_2] [p_2 \leftrightarrow p'_2]} \\ &\quad - \frac{2ig^2}{t} f^{cde} T_{mn}^e r(x_1) z \frac{(z^2/r(x_1))^2 \bar{k} \cdot p_2 + z/r(x_1)(p_3 - p_4) \cdot p_2 - k \cdot p_2)^2}{[(\bar{k} \cdot p_2)/r(x_1)z^2 + (p_3 - x_1 p_4) \cdot p_2 z - x_1 r(x_1) k \cdot p_2] [p_2 \leftrightarrow p'_2]} \\ &\quad \times \left(z(p'_2 - p_2) \cdot (p_3 - x_1 p_4) - x_1 r(x_1) (p'_2 - p_2) \cdot q + z^2/r(x_1) (p'_2 - p_2) \cdot \bar{q} \right) \end{aligned} \tag{77}$$

where the Mandelstam variables are now given by

$$\begin{aligned} s &= (p_1 + p_2)^2 \\ t &= (p_1 + p'_1)^2 = (p_2 + p'_2)^2 \\ u &= (p_1 + p'_2)^2 = (p_2 + p'_1)^2 \end{aligned} \tag{78}$$

where

$$s + t + u = 4m^2. \tag{79}$$

Now, define

$$E^4 \equiv -4(1 - x_1)^2(q \cdot p_2)(\bar{q} \cdot p_2) = -su.$$

and introduce the change in the variables

$$z = \frac{2(1 + x_1)}{E^2} \sqrt{-x_1} (q \cdot p_2) z' = -\frac{2(1 + x_1)}{E^2} \sqrt{-x_1} (q \cdot p'_2) z',$$

to obtain that

$$\begin{aligned} \text{LS}_g^{(s+-)} &= -g^4 \frac{m}{2\sqrt{-t}} \frac{1}{\sqrt{4 - t/m^2}} \left(\frac{N^2 + 2}{4N^2} \delta_{mn} \delta_{ij} + \frac{(N^2 - 4)}{4N} \delta_{mi} \delta_{jn} \right) \\ &\times \frac{1}{2\pi i} \oint_{\Gamma} \frac{dz}{z} \frac{\left(z^2 (-x_1)^{1/2} + \frac{s-u}{E^2} z + \frac{1}{(-x_1)^{1/2}} \right)^2}{\left(1 + \frac{\sqrt{-t}}{m} \frac{u}{E^2} z - z^2 \right) \left(1 - \frac{\sqrt{-t}}{m} \frac{s}{E^2} z - z^2 \right)} \\ &+ \frac{g^4}{4t} \frac{E^2}{(4 - t/m^2)^{3/2}} (N \delta_{mi} \delta_{jn} - \delta_{ij} \delta_{mn}) \\ &\times \frac{1}{2\pi i} \oint_{\Gamma} \frac{dz}{z^2} \frac{\left(z^2 (-x_1)^{1/2} + \frac{s-u}{E^2} z + \frac{1}{(-x_1)^{1/2}} \right)^2 \left(1 + \frac{\sqrt{-t}}{m} \frac{(u-s)}{2E^2} z - z^2 \right)}{\left(1 + \frac{\sqrt{-t}}{m} \frac{u}{E^2} z - z^2 \right) \left(1 - \frac{\sqrt{-t}}{m} \frac{s}{E^2} z - z^2 \right)} \end{aligned} \tag{80}$$

where we used the following $SU(N)$ relation [145]:

$$T_{ml}^c T_{jk}^c = \frac{1}{2} \left(\delta_{mk} \delta_{jl} - \frac{1}{N} \delta_{ml} \delta_{jk} \right). \tag{81}$$

One can also use [145]

$$\begin{aligned} T^c T^d &= \frac{1}{2} \left[\frac{1}{N} \delta^{cd} \mathbf{1} + (d^{cde} + i f^{cde}) T^e \right] \\ f^{abc} f^{abd} &= N \delta^{cd} \\ d^{abc} d^{abd} &= \frac{N^2 - 4}{N} \delta^{cd} \end{aligned} \tag{82}$$

with d^{cde} being the totally symmetric group invariant of $SU(N)$.

Now, let us discuss the choice of the contour Γ . The triangle topology is given by either of the contours that encircles the residues at $z = 0, \infty$. For $\text{LS}_g^{(s+-)}$ we will choose $\Gamma = S_{\infty}^1$. On the other hand, with the replacement $z \rightarrow -1/z$, it is easy to see that we obtain the same integrand as the one for $\text{LS}_g^{(s+-)}$ but with the contour encircling $z = 0$ and in the opposite direction. In other words, the conjugate contribution $\text{LS}_g^{(s-+)}$ is given by $\text{LS}_g^{(s+-)}$ with the replacement $S_{\infty}^1 \rightarrow -S_{\infty}^1$. Finally, enclosing one of the poles produced by the quadratic factors in the denominator will produce the associated box topologies.

The leading singularity associated with the triangle topology is then given by

$$\text{LS}_{\Delta g}^{(s)} = \text{LS}_{\Delta g}^{(s+-)} + \text{LS}_{\Delta g}^{(s-+)} + \text{LS}_{\Delta g}^{(s++)} + \text{LS}_{\Delta g}^{(s--)} \tag{83}$$

where

$$\begin{aligned}
 \text{LS}_{\Delta g}^{(s+-)} + \text{LS}_{\Delta g}^{(s-+)} &= -g^4 \frac{m}{2\sqrt{-t}} \frac{1}{\sqrt{4-t/m^2}} \left(\frac{N^2+2}{4N^2} \delta_{mn} \delta_{ij} + \frac{(N^2-4)}{4N} \delta_{mi} \delta_{jn} \right) \left(-2 + \frac{t}{m^2} \right) \\
 &\quad - \frac{g^4}{8m\sqrt{-t}} \frac{(s-u)}{(4-t/m^2)^{3/2}} (N\delta_{mi} \delta_{jn} - \delta_{ij} \delta_{mn}) \left(-6 + \frac{t}{m^2} \right)
 \end{aligned} \tag{84}$$

and the configurations with equal helicities will not contribute, since

$$\begin{aligned}
 \text{LS}_{\Delta g}^{(s++)} &= \frac{x_1}{4m^2(1-x_1^2)} \frac{1}{2\pi i} \oint_{(s_0^-, s_0^+)} \frac{dz}{z} A_3(\mathbf{1}'_j, \ell, -\ell_1^+) A_3(-\ell, \mathbf{1}_i, -\ell_3^+) A_4(2_m, \ell_3^-, \ell_1^-, 2'_n) \\
 &= \frac{g^4 m^2}{2} \frac{x_1}{(1-x_1^2)} T_{jk}^c T_{ki}^d \frac{1}{2\pi i} \oint_{(s_0^-, s_0^+)} dz \left[\frac{T_{ml}^d T_{ln}^c}{[(\bar{k} \cdot p'_2)z^2 + r(x_1)(p_3 - x_1 p_4) \cdot p'_2 z - x_1 r(x_1)^2 k \cdot p'_2]} \right. \\
 &\quad \left. + \frac{T_{ml}^c T_{ln}^d}{[(\bar{k} \cdot p_2)z^2 + r(x_1)(p_3 - x_1 p_4) \cdot p_2 z - x_1 r(x_1)^2 k \cdot p_2]} \right]
 \end{aligned} \tag{85}$$

and it is clear that this expression has zero residue at both $z = 0, \infty$. A similar result is also valid for $h_1 = h_3 = -1$. Observe the emergence of non-analytic factors in Equation (84)—the second term arises due to the non-Abelian nature of the interaction, which leads to the existence of a physical t -channel massless pole in the Compton amplitude involving gluons. The standard physical interpretation of the two branch points $t = 0$ and $t = 4m^2$ is that they correspond to the threshold for production of massless and massive states. This result agrees with the fact that triangle topology leading singularity is the double discontinuity across the t -channel [55].

As for the box topology, we write

$$\text{LS}_{\square g}^{(s+-)} = \text{LS}_{1\square g}^{(s+-)} + \text{LS}_{2\square g}^{(s+-)} \tag{86}$$

with the following definition:

$$\text{LS}_{1\square g}^{(s+-)} = \frac{2g^4}{t} \frac{x_1^2}{(1-x_1^2)} r(x_1) \frac{1}{4} \left[\delta_{ij} \delta_{mn} \left(1 + \frac{1}{N^2} \right) - \frac{2}{N} \delta_{mi} \delta_{jn} \right] \frac{1}{2\pi i} \oint_{S_{y_0}^1} \frac{dy}{y^2} \frac{\left(-\frac{E^4}{4(1-x_1)^2} y^2 + (p_3 - p_4) \cdot p_2 y - 1 \right)^2}{-\frac{E^4}{4(1-x_1)^2} y^2 + (p_3 - x_1 p_4) \cdot p_2 y - x_1} \tag{87}$$

and $\text{LS}_{2\square g}^{(s+-)}$ can be obtained from $\text{LS}_{1\square g}^{(s+-)}$ by swapping $p_2 \leftrightarrow p'_2$ and $c \leftrightarrow d$ in the Compton amplitude. In the above expression, we performed the change in the variables $z = r(x_1)(q \cdot p_2)y = -r(x_1)(q \cdot p'_2)y$ and we used the definition of E . We also used the Fierz identity again in $SU(N)$. By choosing y_0 to be one of the roots of the denominator, we finally find that

$$\begin{aligned}
 \text{LS}_{1\square g}^{(s+-)} &= \frac{g^4}{16} \left[\left(1 + \frac{1}{N^2} \right) \delta_{ij} \delta_{mn} - \frac{2}{N} \delta_{jn} \delta_{mi} \right] \frac{(u - 2m^2 + \sqrt{E^4 - tu})^2}{t\sqrt{E^4 - tu}} \\
 \text{LS}_{2\square g}^{(s+-)} &= \frac{g^4}{16} \left[\frac{1}{N^2} \delta_{ij} \delta_{mn} + \frac{N^2 - 2}{N} \delta_{jn} \delta_{mi} \right] \frac{(s - 2m^2 + \sqrt{E^4 - ts})^2}{t\sqrt{E^4 - ts}}.
 \end{aligned} \tag{88}$$

One can prove that the reverse helicity configuration can be obtained from the previous expression by taking the other root of the denominator; therefore, with a similar decomposition, we find that

$$\begin{aligned}
 \text{LS}_{1\square g}^{(s-+)} &= \frac{g^4}{16} \left[\left(1 + \frac{1}{N^2} \right) \delta_{ij} \delta_{mn} - \frac{2}{N} \delta_{jn} \delta_{mi} \right] \frac{(u - 2m^2 - \sqrt{E^4 - tu})^2}{t\sqrt{E^4 - tu}} \\
 \text{LS}_{2\square g}^{(s-+)} &= \frac{g^4}{16} \left[\frac{1}{N^2} \delta_{ij} \delta_{mn} + \frac{N^2 - 2}{N} \delta_{jn} \delta_{mi} \right] \frac{(s - 2m^2 - \sqrt{E^4 - ts})^2}{t\sqrt{E^4 - ts}}.
 \end{aligned} \tag{89}$$

Analogous decompositions and calculations for configurations with equal helicity yield

$$\begin{aligned} \text{LS}_{1\Box g}^{(s++)} &= \frac{g^4}{4} \left[\left(1 + \frac{1}{N^2}\right) \delta_{ij} \delta_{mn} - \frac{2}{N} \delta_{jn} \delta_{mi} \right] \frac{m^4}{t\sqrt{E^4 - tu}} \\ \text{LS}_{2\Box g}^{(s++)} &= \frac{g^4}{4} \left[\frac{1}{N^2} \delta_{ij} \delta_{mn} + \frac{N^2 - 2}{N} \delta_{jn} \delta_{mi} \right] \frac{m^4}{t\sqrt{E^4 - ts}}. \end{aligned} \tag{90}$$

It is easy to see that the minus configuration produces the same result. Notice that the box topology yields a pole $1/t$, which would enable one to extend the computation to an r -loop ladder, just as in the gravitational case [55]. Such outcomes are in agreement with the fact that the box topology leading singularity can be envisaged as the discontinuity in the t -channel of the function derived from the calculation of the discontinuity in the s -channel of the one-loop amplitude [55].

Now, let us calculate the one-loop leading singularity with only Merlins in the loop. By using the same method as before, we find that

$$\begin{aligned} \text{LS}_M^{(s)} &= \frac{x_1}{4m^2} \frac{1}{(2\pi i)^3} \oint_{-\Gamma} z dz dA dB \frac{-1}{((2 - M^2/m^2)x_1 + z(Ax_1 + B))} \frac{-1}{((2 - M^2/m^2)x_1 - z(A + Bx_1))} \\ &\times A_3(\mathbf{1}'_j, \ell, -\ell_1) A_3(-\ell, \mathbf{1}_i, -\ell_3) A_4(\mathbf{2}_m, \ell_3, \ell_1, \mathbf{2}'_n) \end{aligned} \tag{91}$$

so that the contour integrations in the A, B planes should be carried out along contours with the opposite direction as the ones taken in the gluon case. Such contour integrations over A, B fix

$$A = -B = \frac{(2 - M^2/m^2)x_1}{z(1 - x_1)} \tag{92}$$

which yields

$$\text{LS}_M^{(s)} = \frac{x_1}{4m^2(1 - x_1^2)} \frac{1}{(2\pi i)} \oint_{\Gamma} \frac{dz}{z} A_3(\mathbf{1}'_j, \ell, -\ell_1) A_3(-\ell, \mathbf{1}_i, -\ell_3) A_4(\mathbf{2}_m, \ell_3, \ell_1, \mathbf{2}'_n). \tag{93}$$

The product of the amplitudes can be evaluated using the results listed above. We choose $\Gamma = S^1_\infty$ to evaluate the triangle leading singularity. We find that

$$\begin{aligned} \text{LS}_{\Delta M}^{(s)} &= -\frac{g^4}{16m} \frac{1}{\sqrt{-t}} \frac{1}{\sqrt{4 - t/m^2}} \left[\left(\frac{N^2 - 2}{N} \delta_{jn} \delta_{mi} + \frac{1}{N^2} \delta_{ij} \delta_{mn} \right) \frac{2M^2u + 2s^2 - st - 2u(t + u)}{(s + u)} \right. \\ &+ \left(\frac{N^2 + 1}{N^2} \delta_{ij} \delta_{mn} - \frac{2}{N} \delta_{jn} \delta_{mi} \right) \frac{2M^2s + 2u^2 - ut - 2s(t + s)}{(s + u)} \\ &+ (N\delta_{mi} \delta_{jn} - \delta_{ij} \delta_{mn}) \frac{(2M^2 + t)(s - u)(-2M^2 + 2s + t + 2u)}{2(s + u)} \left(\frac{1}{t} - \frac{2}{t - M^2} \right) \\ &\left. - \frac{1}{2} \left(\frac{N^2 - 4}{N} \delta_{mi} \delta_{jn} + \frac{N^2 + 2}{N^2} \delta_{ij} \delta_{mn} \right) (t - 8m^2 + 2M^2) \right] \end{aligned} \tag{94}$$

where we used $SU(N)$ identities given above, and the results are

$$\begin{aligned} (p_3 - x_1 p_4) \cdot p_2 &= \frac{r(x_1)}{2} u \\ (p_3 - x_1 p_4) \cdot p'_2 &= \frac{r(x_1)}{2} s \\ p_4 - p_3 &= \frac{p_1 - p'_1}{(1 - x_1)}. \end{aligned} \tag{95}$$

Observe the emergence again of non-analytic factors; there is, however, an important difference here: We verify the presence of the pole at $t = M^2$ due to the presence of the Merlin modes in the t -channel of the Compton amplitude.

As discussed above, the box topology is obtained by considering the poles associated with the roots of the quadratic factors in the denominators. In this case again, we use the definition of E . We obtain

$$\begin{aligned}
 \text{LS}_{\square M}^{(s)} = & -\frac{g^4}{16} \frac{1}{\sqrt{-t}} \left[\left(\frac{N^2 - 2}{N} \delta_{jn} \delta_{mi} + \frac{1}{N^2} \delta_{ij} \delta_{mn} \right) \frac{(4m^2 - M^2 - 2s)^2}{\sqrt{(E^4 - st) \left(u - (t + u) \left(1 - \frac{2M^2}{t+u} \right)^2 \right)}} \right. \\
 & \left. + \left(\frac{N^2 + 1}{N^2} \delta_{ij} \delta_{mn} - \frac{2}{N} \delta_{jn} \delta_{mi} \right) \frac{(4m^2 - M^2 - 2u)^2}{\sqrt{(E^4 - ut) \left(s - (t + s) \left(1 - \frac{2M^2}{t+s} \right)^2 \right)}} \right]. \tag{96}
 \end{aligned}$$

One interesting thing to observe is that the terms associated with the t -channel and the contact term of the Compton amplitude do not contribute to the box leading singularity, only to the triangle one. On the other hand, notice the appearance of the non-analytic factor $\sqrt{-t}$; this is not present in the box topology involving only gluons (which instead develops a pole $1/t$) and is clearly due to the presence of the Merlin modes. Thus, the Merlin particle modifies in a non-trivial way the analytic structure of the amplitude, the crucial difference being the presence of an additional branch cut.

Now, let us calculate the crossed terms. Using the same technique, we find that

$$\begin{aligned}
 \text{LS}_{gM}^{(s)} = & \sum_{h=\pm} \frac{x_1}{4m^2} \frac{1}{(2\pi i)^3} \oint_{-\Gamma} dz dz dA dB \frac{1}{(2x_1 + z(Ax_1 + B))} \frac{-1}{((2 - M^2/m^2)x_1 - z(A + Bx_1))} \\
 & \times A_3(\mathbf{1}'_j, \ell, -\ell_1^h) A_3(-\ell, \mathbf{1}_i, -\ell_3) A_4(\mathbf{2}_m, \ell_3, \ell_1^{-h}, \mathbf{2}'_n) \tag{97}
 \end{aligned}$$

and

$$\begin{aligned}
 \text{LS}_{Mg}^{(s)} = & \sum_{h=\pm} \frac{x_1}{4m^2} \frac{1}{(2\pi i)^3} \oint_{-\Gamma} dz dz dA dB \frac{-1}{((2 - M^2/m^2)x_1 + z(Ax_1 + B))} \frac{1}{(2x_1 - z(A + Bx_1))} \\
 & \times A_3(\mathbf{1}'_j, \ell, -\ell_1) A_3(-\ell, \mathbf{1}_i, -\ell_3^h) A_4(\mathbf{2}_m, \ell_3^{-h}, \ell_1, \mathbf{2}'_n). \tag{98}
 \end{aligned}$$

Carrying out the contour integrations over A and B (taking care to consider proper orientations for the contours as discussed above) yields

$$\text{LS}_{gM}^{(s)} = -\frac{x_1}{4m^2(1 - x_1^2)} \sum_{h=\pm} \frac{1}{(2\pi i)} \oint_{\Gamma} \frac{dz}{z} A_3(\mathbf{1}'_j, \ell, -\ell_1^h) A_3(-\ell, \mathbf{1}_i, -\ell_3) A_4(\mathbf{2}_m, \ell_3, \ell_1^{-h}, \mathbf{2}'_n) \tag{99}$$

with

$$\begin{aligned}
 A_{gM} &= \frac{x_1(M^2 - 2m^2(x_1 + 1))}{m^2(x_1^2 - 1)z} \\
 B_{gM} &= -\frac{x_1(M^2x_1 - 2m^2(x_1 + 1))}{m^2(x_1^2 - 1)z} \tag{100}
 \end{aligned}$$

and

$$\text{LS}_{Mg}^{(s)} = \frac{x_1}{4m^2(1 - x_1^2)} \sum_{h=\pm} \frac{1}{(2\pi i)} \oint_{\Gamma} \frac{dz}{z} A_3(\mathbf{1}'_j, \ell, -\ell_1) A_3(-\ell, \mathbf{1}_i, -\ell_3^h) A_4(\mathbf{2}_m, \ell_3^{-h}, \ell_1, \mathbf{2}'_n) \tag{101}$$

with

$$\begin{aligned}
 A_{Mg} &= \frac{x_1(M^2x_1 - 2m^2(x_1 + 1))}{m^2(x_1^2 - 1)z} = -B_{gM} \\
 B_{Mg} &= -\frac{x_1(M^2 - 2m^2(x_1 + 1))}{m^2(x_1^2 - 1)z} = -A_{gM}. \tag{102}
 \end{aligned}$$

The results presented above allow us to easily calculate the associated product of amplitudes that appear in our expression for the leading singularity associated with the crossed terms. After tedious algebraic manipulations, and again choosing $\Gamma = S_\infty^1$ to evaluate the triangle leading singularity, we find that

$$\begin{aligned} \text{LS}_{\Delta gM}^{(s)} &= \frac{g^4}{8m} \frac{1}{\sqrt{-t}} \frac{1}{\sqrt{4-t/m^2}} \left[\left(\frac{N^2-2}{N} \delta_{jn} \delta_{mi} + \frac{1}{N^2} \delta_{ij} \delta_{mn} \right) (s-2m^2) + \left(\frac{N^2+1}{N^2} \delta_{ij} \delta_{mn} - \frac{2}{N} \delta_{jn} \delta_{mi} \right) (u-2m^2) \right. \\ &- (N\delta_{mi} \delta_{jn} - \delta_{mn} \delta_{ji}) \left(\frac{M^4(u-s) + M^2(s+u)(s-t-u) + t(s-u)(2s+t+2u)}{2(s+u)} \right) \frac{1}{t-M^2} \\ &\left. - \frac{1}{2} \left(\frac{N^2-4}{N} \delta_{mi} \delta_{jn} + \frac{N^2+2}{N^2} \delta_{ij} \delta_{mn} \right) (t-4m^2 + M^2) \right] \end{aligned} \tag{103}$$

and

$$\begin{aligned} \text{LS}_{\Delta Mg}^{(s)} &= -\frac{g^4}{8m} \frac{1}{\sqrt{-t}} \frac{1}{\sqrt{4-t/m^2}} \left[\left(\frac{N^2+1}{N^2} \delta_{ij} \delta_{mn} - \frac{2}{N} \delta_{jn} \delta_{mi} \right) (u-2m^2) + \left(\frac{N^2-2}{N} \delta_{jn} \delta_{mi} + \frac{1}{N^2} \delta_{ij} \delta_{mn} \right) (s-2m^2) \right. \\ &- (N\delta_{mi} \delta_{jn} - \delta_{mn} \delta_{ji}) \left(\frac{M^2(s^2+u(2t-u)) + t(s-u)(2s+t+2u)}{2(s+u)} \right) \frac{1}{t-M^2} \\ &\left. - \frac{1}{2} \left(\frac{N^2-4}{N} \delta_{mi} \delta_{jn} + \frac{N^2+2}{N^2} \delta_{ij} \delta_{mn} \right) (t-4m^2) \right] \end{aligned} \tag{104}$$

where we used

$$(p_4 - p_3 x_1) \cdot p'_2 = \frac{r(x_1)}{2} u.$$

Again observe the appearance of a pole at $t = M^2$.

Now, let us choose a contour encircling one of the poles associated with the roots of the quadratic factors in the denominators. The non-vanishing contribution reads

$$\begin{aligned} \text{LS}_{\square gM}^{(s)} &= \frac{g^4}{4} \frac{\sqrt{(4m^2-t)^2}}{\sqrt{4m^2-t}} \left[\left(\frac{N^2-2}{N} \delta_{jn} \delta_{mi} + \frac{1}{N^2} \delta_{ij} \delta_{mn} \right) \frac{(s-2m^2)^2}{\sqrt{m^2 s (M^2-t)^2 (-st-4u)}} \right. \\ &\left. + \left(\frac{N^2+1}{N^2} \delta_{ij} \delta_{mn} - \frac{2}{N} \delta_{jn} \delta_{mi} \right) \frac{(u-2m^2)^2}{\sqrt{m^2 u (M^2-t)^2 (-ut-4s)}} \right] \end{aligned} \tag{105}$$

and

$$\begin{aligned} \text{LS}_{\square Mg}^{(s)} &= -\frac{g^4}{4} \frac{\sqrt{(4m^2-t)^2}}{\sqrt{4m^2-t}} \left[\left(\frac{N^2+1}{N^2} \delta_{ij} \delta_{mn} - \frac{2}{N} \delta_{jn} \delta_{mi} \right) \frac{(u-2m^2)^2}{\sqrt{m^2 u (M^2-t)^2 (-4s-tu)}} \right. \\ &\left. + \left(\frac{N^2-2}{N} \delta_{jn} \delta_{mi} + \frac{1}{N^2} \delta_{ij} \delta_{mn} \right) \frac{(s-2m^2)^2}{\sqrt{m^2 s (M^2-t)^2 (-4u-ts)}} \right]. \end{aligned} \tag{106}$$

Observe that in principle the crossed terms for the box topology also present non-analytic terms instead of the standard pole $1/t$; however, it is trivial to see that the sum of both contributions vanish, which implies that only the triangle leading singularity is important for such crossed terms—even for the triangle topology, we observe non-trivial cancellations when we sum the two terms above.

4.2. Quadratic Gravity

4.2.1. Graviton Scattering

Now, let us consider the associated gravity leading singularities. We consider a specific one-loop graviton–graviton scattering $h^{++}h^{++} \rightarrow h^{++}h^{++}$. With gravitons running in the loop, we find that the leading singularity is given by

$$LS_h^{(h)} = \sum_{h_1, h_3, h=++,-} \oint_{\Gamma} \frac{d^4 \ell}{(2\pi)^4} \frac{1}{\ell^2(\ell + p'_1)^2(\ell - p_1)^2} M_3(1'^{++}, \ell^{-h}, -\ell_1^{h_1}) M_3(-\ell^h, 1^{++}, -\ell_3^{h_3}) M_4(2^{++}, \ell_3^{-h_3}, \ell_1^{-h_1}, 2'^{++}). \quad (107)$$

For Merlins running in the loop, we find that

$$LS_M^{(h)} = \oint_{-\Gamma} \frac{d^4 \ell}{(2\pi)^4} \frac{-1}{(\ell^2 - M^2)} \frac{-1}{[(\ell + p'_1)^2 - M^2]} \frac{-1}{[(\ell - p_1)^2 - M^2]} M_3(1'^{++}, \ell, -\ell_1) M_3(-\ell, 1^{++}, -\ell_3) M_4(2^{++}, \ell_3, \ell_1, 2'^{++}). \quad (108)$$

The double-copy prescription allows us to recycle the gluon results derived previously, and we find that $LS_h^{(h)} = 0$. Essentially the reason is the same as before: A similar supersymmetric decomposition allows one to see that the one-loop scattering amplitude $M_4^{1-loop}[1'^{++}, 1^{++}, 2^{++}, 2'^{++}]$ consists of purely rational terms, which are cut-free in four dimensions [146]. Hence, the associated leading singularity must be zero in four dimensions.

For the case of Merlins running in the loop, we will need the double-copy results presented above, and will also need to take the adequate orientation for the associated contours; proceeding as in the analogous gauge-theory case, we find that

$$\begin{aligned} LS_M^{(h)} &= -\frac{1}{8(p_1 \cdot p'_1)} \frac{1}{(2\pi i)} \oint_{\Gamma} \frac{dz}{z} M_3(1'^{++}, \ell, -\ell_1) M_3(-\ell, 1^{++}, -\ell_3) M_4(2^{++}, \ell_3, \ell_1, 2'^{++}) \\ &= -\left(\delta_I^{(I} \delta_J^J \delta_K^K \delta_L^{L)}\right) \frac{2iM^8}{(p_1 \cdot p'_1)} \frac{[22']^2 [11']^2}{\langle 22' \rangle^2 \langle 11' \rangle^2} \frac{1}{(2\pi i)} \oint_{\Gamma} \frac{dz}{z} \left(\frac{1}{2p'_2 \cdot \ell_1} + \frac{1}{2p_2 \cdot \ell_1} \right) \\ &= iM^8 \left(\delta_I^{(I} \delta_J^J \delta_K^K \delta_L^{L)}\right) \frac{[22']^2 [11']^2}{\langle 22' \rangle^2 \langle 11' \rangle^2} \frac{1}{(2\pi i)} \oint_{\Gamma} \frac{dz}{z} \left(\frac{2z}{-2(p_1 \cdot p'_1)(\bar{q} \cdot p'_2)z^2 - 2(p_1 \cdot p'_1)(p'_1 \cdot p'_2)z + M^2 q \cdot p'_2} \right. \\ &\quad \left. + \frac{2z}{-2(p_1 \cdot p'_1)(\bar{q} \cdot p_2)z^2 - 2(p_1 \cdot p'_1)(p'_1 \cdot p_2)z + M^2 q \cdot p_2} \right). \end{aligned} \quad (109)$$

In [87] a similar product of amplitudes was considered, except that the result in there lacks the above overall factor given by a (non-normalized) symmetric product of the delta functions, so this expression slightly corrects the analogous one in such a reference. As in previous case, we see that $LS_{\Delta M}^{(h)} = 0$. The box topology can be easily calculated by relying on the results derived above:

$$LS_{\square M}^{(h)} = \left(\delta_I^{(I} \delta_J^J \delta_K^K \delta_L^{L)}\right) \frac{i\kappa^4 M^8}{4} \left(\frac{ut}{\langle 11' \rangle \langle 1'2 \rangle \langle 22' \rangle \langle 2'1 \rangle} \right)^2 \left(\frac{1}{\sqrt{s^2 u^2 + 4M^2 stu}} + \frac{1}{\sqrt{t^2 u^2 + 4M^2 stu}} \right) \quad (110)$$

where the Mandelstam variables are defined as $s = (p_1 + p_2)^2$, $t = (p_1 + p'_2)^2$ and $u = (p_1 + p'_1)^2$, with $s + t + u = 0$. We also restored the factors $\kappa/2$ coming from the amplitudes. As in the previous case, in the one-loop amplitude only the box integral is present [87]—as a result, only the box topology is non-vanishing.

4.2.2. Scalar Scattering

To conclude our exploration, let us now study leading singularities in the scattering of identical scalar particles $\phi\phi \rightarrow \phi\phi$ interacting gravitationally. The associated expressions are given by

$$LS_h^{(s)} = \sum_{h_1, h_3=++,-} \oint_{\Gamma} \frac{d^4 \ell}{(2\pi)^4} \frac{1}{(\ell^2 - m^2)} \frac{1}{(\ell + p'_1)^2(\ell - p_1)^2} M_3(\mathbf{1}', \ell, -\ell_1^{h_1}) M_3(-\ell, \mathbf{1}, -\ell_3^{h_3}) M_4(\mathbf{2}, \ell_3^{-h_3}, \ell_1^{-h_1}, \mathbf{2}') \quad (111)$$

for gravitons running in the loop, whereas for Merlins we find that

$$LS_M^{(s)} = \oint_{-\Gamma} \frac{d^4 \ell}{(2\pi)^4} \frac{-1}{(\ell^2 - m^2)} \frac{-1}{[(\ell + p'_1)^2 - M^2]} \frac{-1}{[(\ell - p_1)^2 - M^2]} M_3(\mathbf{1}', \ell, -\ell_1) M_3(-\ell, \mathbf{1}, -\ell_3) M_4(\mathbf{2}, \ell_3, \ell_1, \mathbf{2}') \quad (112)$$

where m is the mass of the scalar particles. We consider all possible Merlins here—the ones associated with the graviton, the dilaton and the Kalb–Ramond fields. This amounts to taking the total Merlin propagator in the form

$$D_{\mu\rho;\nu\sigma}(p)\Big|_{\text{Merlin}} = -\frac{1}{(p^2 - M^2)}\tilde{\pi}_{\mu\rho}\tilde{\pi}_{\nu\sigma} \tag{113}$$

which would only contract “left” indices with “right” indices. Three-point vertices would also have to be constructed in this way, as a product of three-point (higher-derivative) Yang–Mills vertices. Such a factorization would make the double-copy property manifest. Similar choices for the graviton propagator and the associated three-point vertex were proposed in [147].

As above, one also has to consider two crossed terms:

$$\begin{aligned} \text{LS}_{hM}^{(s)} &= \sum_h \oint_{-\Gamma} \frac{d^4\ell}{(2\pi)^4(\ell^2 - m^2)} \frac{1}{(\ell + p_1')^2} \frac{-1}{[(\ell - p_1)^2 - M^2]} M_3(\mathbf{1}', \ell, -\ell_1^h) M_3(-\ell, \mathbf{1}, -\ell_3) M_4(\mathbf{2}, \ell_3, \ell_1^{-h}, \mathbf{2}') \\ \text{LS}_{Mh}^{(s)} &= \sum_h \oint_{-\Gamma} \frac{d^4\ell}{(2\pi)^4(\ell^2 - m^2)} \frac{-1}{[(\ell + p_1')^2 - M^2]} \frac{1}{(\ell - p_1)^2} M_3(\mathbf{1}', \ell, -\ell_1) M_3(-\ell, \mathbf{1}, -\ell_3^h) M_4(\mathbf{2}, \ell_3^{-h}, \ell_1, \mathbf{2}') \end{aligned} \tag{114}$$

which contain a four-point amplitude with external Merlin and graviton, in addition to the scalars. Observe that in such crossed terms all degrees of freedom generated by the double-copy procedure are being taken into account. Concerning the graviton contribution, this would be equivalent to taking its propagator in the double-copy form [147]

$$D_{\mu\rho;\nu\sigma}(p)\Big|_{\text{graviton}} = \frac{1}{p^2}\eta_{\mu\rho}\eta_{\nu\sigma} \tag{115}$$

and the terminology “graviton” above could apply to all massless degrees of freedom produced by the double copy—unless we impose that all vertices in the n -graviton scattering amplitude should satisfy a rigid left–right interchange symmetry, as explained in [147]. As in the gauge-theory case, there are also other contributions that can be obtained from those above by considering $1 \leftrightarrow 2$.

Let us begin with the case of only gravitons running in the loop. Since this was already calculated before, we simply quote the result [55]. For the triangle topology, we find that

$$\text{LS}_{\Delta h}^{(s)} = \text{LS}_{\Delta h}^{(s++,--)} + \text{LS}_{\Delta h}^{(s--,++)} + \text{LS}_{\Delta h}^{(s++,++)} + \text{LS}_{\Delta h}^{(s--,--)} \tag{116}$$

where

$$\text{LS}_{\Delta h}^{(s++,--)} + \text{LS}_{\Delta h}^{(s--,++)} = i\left(\frac{\kappa}{2}\right)^4 \frac{m}{\sqrt{-t}} \frac{m^4}{(4 - t/m^2)^{5/2}} \frac{1}{2\pi i} \oint_{(s_1^\infty - s_0^1)} \frac{dz}{z^3} \frac{\left(z^2(-x_1)^{1/2} + \frac{s-u}{E^2}z + \frac{1}{(-x_1)^{1/2}}\right)^4}{\left(1 + \frac{\sqrt{-t}}{m} \frac{u}{E^2}z - z^2\right)\left(1 - \frac{\sqrt{-t}}{m} \frac{s}{E^2}z - z^2\right)} \tag{117}$$

and the contributions with equal helicities vanish. The box topology can be calculated in much the same way as was done in the Yang–Mills case; the final result reads

$$\text{LS}_{\square h}^{(s)} = \text{LS}_{\square h}^{(s++,--)} + \text{LS}_{\square h}^{(s--,++)} + \text{LS}_{\square h}^{(s++,++)} + \text{LS}_{\square h}^{(s--,--)} \tag{118}$$

with

$$\begin{aligned} \text{LS}_{\square h}^{(s++,--)} &= iG^2\pi^2 \frac{(s - 2m^2 + \sqrt{E^4 - ts})^4}{t\sqrt{E^4 - ts}} \\ \text{LS}_{\square h}^{(s--,++)} &= G^2\pi^2 \frac{(s - 2m^2 - \sqrt{E^4 - ts})^4}{t\sqrt{E^4 - ts}} \end{aligned} \tag{119}$$

and

$$LS_{\square h}^{(s+,+,+)} = LS_{\square h}^{(s--,--)} = iG^2\pi^2 \frac{m^8}{t\sqrt{E^4-ts}}. \tag{120}$$

Now, let us evaluate the one-loop leading singularity with only gravitational Merlins in the loop. By using the same technique as above, we find that

$$LS_M^{(s)} = \frac{x_1}{4m^2(1-x_1^2)} \frac{1}{(2\pi i)} \oint_{\Gamma} \frac{dz}{z} M_3(\mathbf{1}', \ell, -\ell_1) M_3(-\ell, \mathbf{1}, -\ell_3) M_4(\mathbf{2}, \ell_3, \ell_1, \mathbf{2}') \tag{121}$$

with

$$A = -B = \frac{(2 - M^2/m^2)x_1}{z(1-x_1)}. \tag{122}$$

Using the double-copy prescription enables one to derive simple expressions for the product of the amplitudes that enter in the above formula. We stress again that we are taking into account all the degrees of freedom comprised of the double copy, that is, gravitons, Merlins, dilatons and Kalb–Ramonds. In order to consider only gravitons and gravitational Merlins, one must disentangle them from the other contributions—this is achieved by using the four-dimensional physical state projectors given above. In any case, all terms above will contribute to the triangle leading singularity. By taking $\Gamma = S_{\infty}^1$, we find that

$$\begin{aligned} LS_{\Delta M}^{(s)} &= \frac{i\kappa^4}{4m} \frac{1}{\sqrt{-t}} \frac{1}{\sqrt{4-t/m^2}} \frac{1}{(2\pi i)} \oint_{S_{\infty}^1} \frac{dy}{y} \left\{ - \left[\left(s - 2m^2 - \frac{1}{2}(S(y) + M^2) \right)^2 + \frac{1}{8}(-8m^2 + 2M^2 + t)S(y) \right]^2 \frac{1}{S(y)} \right. \\ &- \left[\left(u - 2m^2 - \frac{1}{2}(U(y) - M^2) \right)^2 + \frac{1}{8}(-8m^2 + 2M^2 + t)U(y) \right]^2 \frac{1}{U(y)} \\ &+ \left. \left(\frac{1}{8}(-8m^2 + 2M^2 + 3t)(S(y) - U(y)) - \frac{t}{2}(s - u - M^2) \right)^2 \left(\frac{1}{t} - \frac{2}{t - M^2} \right) \right\} \end{aligned} \tag{123}$$

where

$$\begin{aligned} S(y) &= \frac{1}{y} \left(\frac{E^4 r(x_1)}{2(1-x_1)^2} y^2 + \frac{s(2M^2-t)}{s+u} y + 2r(x_1)x_1 \left(1 + \frac{(M^2-4m^2)M^2}{m^2 t} \right) \right) \\ U(y) &= \frac{1}{y} \left(-\frac{E^4 r(x_1)}{2(1-x_1)^2} y^2 + \frac{u(2M^2-t)}{s+u} y - 2r(x_1)x_1 \left(1 + \frac{(M^2-4m^2)M^2}{m^2 t} \right) \right) \end{aligned} \tag{124}$$

and we used the change of variables $z = r(x_1)(q \cdot p_2)y = -r(x_1)(q \cdot p'_2)y$. The Mandelstam variables are now given by Equation (78). The contour integral is not terribly difficult to solve; however, the explicit result is not particularly enlightening, so we choose to leave it in such a compact form. Nevertheless, we can check from the above expression the emergence of the standard non-analytic terms $1/\sqrt{-t}$ and $1/\sqrt{4-t/m^2}$ for triangle topologies, together with the pole at $t = M^2$, which is a typical feature due to the presence of Merlin modes.

To compute the box topology, we proceed as before; that is, we consider a contour encircling one of the poles associated with the roots of the quadratic factors in the denominators. We obtain

$$LS_{\square M}^{(s)} = -i \left(\frac{\kappa}{2} \right)^4 \frac{1}{4\sqrt{-t}} \left[\frac{(4m^2 - M^2 - 2s)^4}{\sqrt{(E^4 - st) \left(u - (t+u) \left(1 - \frac{2M^2}{t+u} \right)^2 \right)}} + \frac{(4m^2 - M^2 - 2u)^4}{\sqrt{(E^4 - ut) \left(s - (t+s) \left(1 - \frac{2M^2}{t+s} \right)^2 \right)}} \right]. \tag{125}$$

As in the Yang–Mills case, Merlin modes change dramatically the analytic structure of the amplitude—in the present case, this non-trivial change means that, instead of the $1/t$

pole for the box topology found in the case of gravitons running in the loop, we find the non-analytic term $\sqrt{-t}$.

Now, let us calculate the crossed terms. Using the same technique as above, we find that

$$LS_{hM}^{(s)} = -\frac{x_1}{4m^2(1-x_1^2)} \sum_h \frac{1}{(2\pi i)} \oint_{\Gamma} \frac{dz}{z} M_3(\mathbf{1}', \ell, -\ell_1^h) M_3(-\ell, \mathbf{1}, -\ell_3) M_4(\mathbf{2}, \ell_3, \ell_1^{-h}, \mathbf{2}') \tag{126}$$

with the associated A and B given by Equation (100) and

$$LS_{Mh}^{(s)} = \frac{x_1}{4m^2(1-x_1^2)} \sum_h \frac{1}{(2\pi i)} \oint_{\Gamma} \frac{dz}{z} M_3(\mathbf{1}', \ell, -\ell_1) M_3(-\ell, \mathbf{1}, -\ell_3^h) M_4(\mathbf{2}, \ell_3^{-h}, \ell_1, \mathbf{2}') \tag{127}$$

and now A and B are given by Equation (102). In turn, the amplitudes listed above allow us to calculate the products of the amplitudes that appear in both expressions. As above, we take $\Gamma = S_{\infty}^1$ for the calculation of the triangle topology. Performing the same change in the variables as above, we find that

$$\begin{aligned} LS_{hM}^{(s)} &= 16i \left(\frac{\kappa}{2}\right)^4 \frac{1}{4m} \frac{1}{\sqrt{-t}} \frac{1}{\sqrt{4-t/m^2}} \frac{1}{(2\pi i)} \oint_{S_{\infty}^1} \frac{dy}{y} \left\{ \left[\left(s - 2m^2 - \frac{1}{2} \mathcal{S}(y) \right) (s - 2m^2) + \frac{(t - 4m^2 + M^2)}{4} \mathcal{S}(y) \right]^2 \frac{1}{\mathcal{S}(y)} \right. \\ &+ \left[\left(u - 2m^2 - \frac{1}{2} \mathcal{U}(y) \right) (u - 2m^2) + \frac{(t - 4m^2 + M^2)}{4} \mathcal{U}(y) \right]^2 \frac{1}{\mathcal{U}(y)} \\ &+ \left. \left[\frac{(t - 4m^2 + M^2)}{4} (\mathcal{S}(y) - \mathcal{U}(y)) + \frac{t}{2} \mathcal{S}(y) + \frac{1}{4} t(-3s + t + 3u) \right]^2 \frac{1}{t - M^2} \right\} \end{aligned} \tag{128}$$

and

$$\begin{aligned} LS_{Mh}^{(s)} &= -16i \left(\frac{\kappa}{2}\right)^4 \frac{1}{4m} \frac{1}{\sqrt{-t}} \frac{1}{\sqrt{4-t/m^2}} \frac{1}{(2\pi i)} \oint_{S_{\infty}^1} \frac{dy}{y} \\ &\times \left\{ \left[\left(u - 2m^2 - \frac{1}{2} \mathcal{U}(y) \right) (u - 2m^2) + \frac{(t - 4m^2)}{4} \mathcal{U}(y) \right]^2 \frac{1}{\mathcal{U}(y)} \right. \\ &+ \left[\left(s - 2m^2 - \frac{1}{2} \mathcal{S}(y) \right) (s - 2m^2) + \frac{(t - 4m^2)}{4} \mathcal{S}(y) \right]^2 \frac{1}{\mathcal{S}(y)} \\ &+ \left. \left[\frac{t}{2} (\mathcal{S}(y) - \mathcal{U}(y)) - 2m^2 \mathcal{S}(y) - \frac{1}{4} t(4s + t - 2u) - \frac{M^2}{4} (t - 4m^2) \right]^2 \frac{1}{t - M^2} \right\} \end{aligned} \tag{129}$$

where

$$\begin{aligned} \mathcal{S}(y) &= \frac{1}{y} \left(-\frac{(t - M^2)}{s + u} sy + \frac{E^4}{2(1 - x_1)^2} r(x_1) y^2 + 2r(x_1) x_1 \frac{(t - M^2)^2}{t^2} \right) \\ \mathcal{U}(y) &= \frac{1}{y} \left(-\frac{(t - M^2)}{s + u} uy - \frac{E^4}{2(1 - x_1)^2} r(x_1) y^2 - 2r(x_1) x_1 \frac{(t - M^2)^2}{t^2} \right). \end{aligned} \tag{130}$$

Again, the emergence of the non-standard pole at $t = M^2$ is manifest.

The box topology for the crossed terms can be calculated in much the same way as before; we obtain that

$$LS_{\square hM}^{(s)} = \frac{ik^4}{4} \frac{\sqrt{(4m^2 - t)^2}}{\sqrt{4m^2 - t}} \left[\frac{(s - 2m^2)^4}{\sqrt{m^2 s (M^2 - t)^2 (-st - 4u)}} + \frac{(u - 2m^2)^4}{\sqrt{m^2 u (M^2 - t)^2 (-ut - 4s)}} \right] \tag{131}$$

and

$$LS_{\square Mh}^{(s)} = -\frac{ik^4}{4} \frac{\sqrt{(4m^2 - t)^2}}{\sqrt{4m^2 - t}} \left[\frac{(u - 2m^2)^4}{\sqrt{m^2 u (M^2 - t)^2 (-4s - tu)}} + \frac{(s - 2m^2)^4}{\sqrt{m^2 s (M^2 - t)^2 (-4u - ts)}} \right]. \tag{132}$$

Similar to the gauge-theory case, the sum of both contributions also vanishes.

5. Summary

Unitarity cut enables one to establish a relationship between the pole structure of the integrand and the branch-cut structure of the loop integral. This allows one to retrieve the loop integrand by analyzing different sets of unitarity cuts. It turns out that the problem of finding functions which can reproduce all such discontinuities can be a daunting endeavor. We have studied here one special class of such singularities, the leading singularities, which are the ones with the highest co-dimension. We have investigated leading singularities in a higher-derivative Yang–Mills theory and quadratic gravity. As shown in previous sections, this technique can still be a powerful one to address the reconstruction of loop amplitudes for such theories. Indeed, the applicability of unitarity-based methods to amplitudes involving unstable particles can be envisaged as a consequence of unitarity. As proved in [59,64], theories with unstable particles are unitary. Therefore, unitarity methods must be trustworthy in such cases. This is extensively discussed in [69]. In turn, when computing leading singularities, the associated contours must enclose one-particle poles so that the result of the contour integration will represent an on-shell particle carrying positive energy. In the case of unstable particles, when one is off resonance, one is also away from the pole of the propagator, and one obtains a vanishing residue. Hence, a finite result is only warranted when one is close to the resonance region.

The present study is a natural continuation of the investigation initiated in [69,87], where the analytic properties of scattering amplitudes of higher-derivative field theories were approached. This is an important point as it is well known that resummed Merlin propagators do not satisfy standard analyticity properties since the poles are on the physical sheet, which leads to an unorthodox analytic structure for the associated amplitudes. Indeed, as shown by the calculations above, the presence of Merlin modes alters the form of the box leading singularities in a non-trivial way. Our results suggest that a better understanding of the analytic features of the amplitudes calculated in such theories is a pressing issue. The use of tools coming from the modern on-shell amplitudes program seems to be a promising pathway to be explored.

It is unclear whether traditional field-theory techniques agree in their results when applied to higher-derivative theories. For instance, the equivalence of Euclidean and Lorentzian formulations has been grounded in standard theories, and it is not clear how such a correspondence would be possible for higher-derivative theories, particularly bearing mind the unconventional analytic features such theories possess [61]. Perhaps the traditional representation of loop amplitudes in terms of Feynman diagrams might not be useful here. It is known that in many situations the Lee–Wick contour is mandatory; however, one is unsure of the consistency of this prescription to higher orders in perturbation theory [78–83]. In turn, it is also unclear how to include the CLOP prescription into a Lagrangian, and ambiguities are expected to arise at higher orders [148]. Standard Feynman diagrams were originally conceived for theories with scattering amplitudes which are analytic in the first Riemann sheet, and models enjoying one unambiguous arrow of causality. This is not the case here. An alternative treatment could probe other options; perhaps recent ideas comprising representations of amplitudes in terms of contour integrals in Grassmannian spaces or geometrizations such as amplituhedrons could be helpful here [51,149–153]. On the other hand, as discussed, gravitational scattering amplitudes can be written as an appropriate factorization in terms of gauge-theory amplitudes. The conjecture is that the double copy might be a general imprint of all gravitational theories. The current study as well as the investigation put forward in [87] were restricted to examining in detail four-point amplitudes in quadratic gravity; it would be interesting to see more evidence in favor of a double-copy structure with five- or higher-point amplitudes. These are certainly explorations worthy of further consideration within the program of quadratic gravity as a potential UV completion for quantum gravity, and we hope to return to such considerations in the near future.

Funding: This work has been partially supported by Conselho Nacional de Desenvolvimento Científico e Tecnológico—CNPq under grant 317548/2021-2 and Fundação Carlos Chagas Filho de Amparo à Pesquisa do Estado do Rio de Janeiro—FAPERJ under grants E-26/202.725/2018 and E-26/201.142/2022.

Institutional Review Board Statement: Not applicable.

Informed Consent Statement: Not applicable.

Data Availability Statement: Not applicable.

Conflicts of Interest: The author declares no conflict of interest.

Notes

- ¹ For a much more extensive body of research on unitarity-based methods, please check references within [2,15–50].
- ² For this calculation one can make use of the triple-gauge vertex calculated in detail in [87].

References

1. Witten, E. Perturbative gauge theory as a string theory in twistor space. *Commun. Math. Phys.* **2004**, *252*, 189–258. [[CrossRef](#)]
2. Britto, R.; Cachazo, F.; Feng, B. Generalized unitarity and one-loop amplitudes in $N = 4$ super-Yang–Mills. *Nucl. Phys. B* **2005**, *725*, 275–305. [[CrossRef](#)]
3. Arkani-Hamed, N.; Cachazo, F.; Kaplan, J. What is the Simplest Quantum Field Theory? *J. High Energy Phys.* **2010**, *2010*, 16. [[CrossRef](#)]
4. Arkani-Hamed, N.; Bourjaily, J.; Cachazo, F.; Trnka, J. Unification of Residues and Grassmannian Dualities. *J. High Energy Phys.* **2011**, *2011*, 49. [[CrossRef](#)]
5. Arkani-Hamed, N.; Bourjaily, J.L.; Cachazo, F.; Caron-Huot, S.; Trnka, J. The All-Loop Integrand For Scattering Amplitudes in Planar $N = 4$ SYM. *J. High Energy Phys.* **2011**, *2011*, 41. [[CrossRef](#)]
6. Arkani-Hamed, N.; Bourjaily, J.L.; Cachazo, F.; Goncharov, A.B.; Postnikov, A.; Trnka, J. *Scattering Amplitudes and the Positive Grassmannian*; Cambridge University Press: Cambridge, UK, 2016.
7. Eden, R.J.; Landshoff, P.V.; Olive, D.I.; Polkinghorne, J.C. *The Analytic S-Matrix*; Cambridge University Press: Cambridge, UK, 1966.
8. Weinberg, S. Feynman Rules for Any Spin. 2. Massless Particles. *Phys. Rev.* **1964**, *134*, B882–B896. [[CrossRef](#)]
9. Weinberg, S. Photons and Gravitons in S-Matrix Theory: Derivation of Charge Conservation and Equality of Gravitational and Inertial Mass. *Phys. Rev.* **1964**, *135*, B1049–B1056. [[CrossRef](#)]
10. Weinberg, S. Photons and gravitons in perturbation theory: Derivation of Maxwell’s and Einstein’s equations. *Phys. Rev.* **1965**, *138*, B988–B1002. [[CrossRef](#)]
11. Olive, D.I. Exploration of S-Matrix Theory? *Phys. Rev.* **1964**, *135*, B745–B760. [[CrossRef](#)]
12. Chew, G.F. *The Analytic S-Matrix: A Basis for Nuclear Democracy?* W. A. Benjamin, Inc.: New York, NY, USA, 1966.
13. Cutkosky, R.E. Singularities and discontinuities of Feynman amplitudes. *J. Math. Phys.* **1960**, *1*, 429–433. [[CrossRef](#)]
14. Schwartz, M.D. *Quantum Field Theory and the Standard Model*; Cambridge University Press: Cambridge, UK, 2013.
15. Bern, Z.; Dixon, L.J.; Dunbar, D.C.; Kosower, D.A. One loop n point gauge theory amplitudes, unitarity and collinear limits. *Nucl. Phys. B* **1994**, *425*, 217–260. [[CrossRef](#)]
16. Bern, Z.; Dixon, L.J.; Dunbar, D.C.; Kosower, D.A. Fusing gauge theory tree amplitudes into loop amplitudes. *Nucl. Phys. B* **1995**, *435*, 59–101. [[CrossRef](#)]
17. Bern, Z.; Morgan, A.G. Massive loop amplitudes from unitarity. *Nucl. Phys. B* **1996**, *467*, 479–509. [[CrossRef](#)]
18. Bern, Z.; Dixon, L.J.; Kosower, D.A. Progress in one loop QCD computations. *Ann. Rev. Nucl. Part. Sci.* **1996**, *46*, 109–148. [[CrossRef](#)]
19. Bern, Z.; Dixon, L.J.; Dunbar, D.C.; Kosower, D.A. One loop selfdual and $N = 4$ superYang–Mills. *Phys. Lett. B* **1997**, *394*, 105–115. [[CrossRef](#)]
20. Bern, Z.; Dixon, L.J.; Kosower, D.A. One loop amplitudes for $e^+ e^-$ to four partons. *Nucl. Phys. B* **1998**, *513*, 3–86. [[CrossRef](#)]
21. Bern, Z.; Dixon, L.J.; Kosower, D.A. Two-loop $g \rightarrow gg$ splitting amplitudes in QCD. *J. High Energy Phys.* **2004**, *2004*, 12. [[CrossRef](#)]
22. Forde, D. Direct extraction of one-loop integral coefficients. *Phys. Rev. D* **2007**, *75*, 125019. [[CrossRef](#)]
23. Kosower, D.A.; Larsen, K.J. Maximal unitarity at two loops. *Phys. Rev. D* **2012**, *85*, 045017. [[CrossRef](#)]
24. Caron-Huot, S.; Larsen, K.J. Uniqueness of two-loop master contours. *J. High Energy Phys.* **2012**, *2012*, 26. [[CrossRef](#)]
25. Johansson, H.; Kosower, D.A.; Larsen, K.J. Two-Loop Maximal Unitarity with External Masses. *Phys. Rev. D* **2013**, *87*, 025030. [[CrossRef](#)]
26. Johansson, H.; Kosower, D.A.; Larsen, K.J. Maximal Unitarity for the Four-Mass Double Box. *Phys. Rev. D* **2014**, *89*, 125010. [[CrossRef](#)]
27. Abreu, S.; Britto, R.; Duhr, C.; Gardi, E. Cuts from residues: The one-loop case. *J. High Energy Phys.* **2017**, *2017*, 114. [[CrossRef](#)]
28. Sogaard, M.; Zhang, Y. Elliptic Functions and Maximal Unitarity. *Phys. Rev. D* **2015**, *91*, 081701. [[CrossRef](#)]

29. Larsen, K.J.; Zhang, Y. Integration-by-parts reductions from unitarity cuts and algebraic geometry. *Phys. Rev. D* **2016**, *93*, 041701. [[CrossRef](#)]
30. Ita, H. Two-loop Integrand Decomposition into Master Integrals and Surface Terms. *Phys. Rev. D* **2016**, *94*, 116015. [[CrossRef](#)]
31. Remiddi, E.; Tancredi, L. Differential equations and dispersion relations for Feynman amplitudes. The two-loop massive sunrise and the kite integral. *Nucl. Phys. B* **2016**, *907*, 400. [[CrossRef](#)]
32. Primo, A.; Tancredi, L. On the maximal cut of Feynman integrals and the solution of their differential equations. *Nucl. Phys. B* **2017**, *916*, 94–116. [[CrossRef](#)]
33. Frellesvig, H.; Papadopoulos, C.G. Cuts of Feynman Integrals in Baikov representation. *J. High Energy Phys.* **2017**, *2017*, 83. [[CrossRef](#)]
34. Zeng, M. Differential equations on unitarity cut surfaces. *J. High Energy Phys.* **2017**, *2017*, 121. [[CrossRef](#)]
35. Ellis, R.K.; Kunszt, Z.; Melnikov, K.; Zanderighi, G. One-loop calculations in quantum field theory: From Feynman diagrams to unitarity cuts. *Phys. Rep.* **2012**, *518*, 141–250. [[CrossRef](#)]
36. Frellesvig, H.A. Generalized Unitarity Cuts and Integrand Reduction at Higher Loop Orders. Ph.D. Thesis, Faculty of Science, University of Copenhagen, Copenhagen, Denmark, 2014.
37. Brandhuber, A.; McNamara, S.; Spence, B.; Travaglini, G. Loop amplitudes in pure Yang–Mills from generalised unitarity. *J. High Energy Phys.* **2005**, *2005*, 11. [[CrossRef](#)]
38. Britto, R. Loop Amplitudes in Gauge Theories: Modern Analytic Approaches. *J. Phys. A* **2011**, *44*, 454006. [[CrossRef](#)]
39. Carrasco, J.J.M.; Johansson, H. Generic multiloop methods and application to $\mathcal{N} = 4$ super-Yang–Mills. *J. Phys. A Math. Theor.* **2011**, *44*, 454004. [[CrossRef](#)]
40. Abreu, S.; Britto, R.; Grönqvist, H. Cuts and coproducts of massive triangle diagrams. *J. High Energy Phys.* **2015**, *2015*, 111. [[CrossRef](#)]
41. Bern, Z.; Duca, V.D.; Dixon, L.J.; Kosower, D.A. All non-maximally-helicity-violating one-loop seven-gluon amplitudes in $N = 4$ super-yang-Mills theory. *Phys. Rev. D* **2005**, *71*, 045006. [[CrossRef](#)]
42. Britto, R.; Feng, B.; Mastrolia, P. Closed-Form Decomposition of One-Loop Massive Amplitudes. *Phys. Rev. D* **2008**, *78*, 025031. [[CrossRef](#)]
43. Bern, Z.; Huang, Y.-T. Basics of generalized unitarity. *J. Phys. A Math. Theor.* **2011**, *44*, 454003. [[CrossRef](#)]
44. Bern, Z.; Carrasco, J.J.; Dennen, T.; Huang, Y.t.; Ita, H. Generalized Unitarity and Six-Dimensional Helicity. *Phys. Rev. D* **2011**, *83*, 085022. [[CrossRef](#)]
45. Drummond, J.M.; Henn, J.; Korchemsky, G.P.; Sokatchev, E. Generalized unitarity for $N = 4$ super-amplitudes. *Nucl. Phys. B* **2013**, *869*, 452–492. [[CrossRef](#)]
46. Engelund, O.T.; McKeown, R.W.; Roiban, R. Generalized unitarity and the worldsheet S matrix in $AdS_n \times S^n \times M^{10-2n}$. *J. High Energy Phys.* **2013**, *2013*, 23. [[CrossRef](#)]
47. Elvang, H.; Hadjiantonis, M.; Jones, C.R.T.; Paranjape, S. All-Multiplicity One-Loop Amplitudes in Born-Infeld Electrodynamics from Generalized Unitarity. *J. High Energy Phys.* **2020**, *2020*, 9. [[CrossRef](#)]
48. Bern, Z.; Kosmopoulos, D.; Zhiboedov, A. Gravitational effective field theory islands, low-spin dominance, and the four-graviton amplitude. *J. Phys. A* **2021**, *54*, 344002. [[CrossRef](#)]
49. Bern, Z.; Parra-Martinez, J.; Sawyer, E. Structure of two-loop SMEFT anomalous dimensions via on-shell methods. *J. High Energy Phys.* **2020**, *2020*, 211. [[CrossRef](#)]
50. Primo, A.; Bobadilla, W.J.T. BCJ Identities and d -Dimensional Generalized Unitarity. *J. High Energy Phys.* **2016**, *2016*, 125. [[CrossRef](#)]
51. Elvang, H.; Huang, Y.-T. *Scattering Amplitudes in Gauge Theory and Gravity*; Cambridge University Press: Cambridge, UK, 2015.
52. Buchbinder, E.I.; Cachazo, F. Two-loop amplitudes of gluons and octa-cuts in $N = 4$ super Yang–Mills. *J. High Energy Phys.* **2005**, *2005*, 36. [[CrossRef](#)]
53. Cachazo, F.; Skinner, D. On the structure of scattering amplitudes in $N = 4$ super Yang–Mills and $N = 8$ supergravity. *arXiv* **2008**, arXiv:0801.4574.
54. Cachazo, F. Sharpening The Leading Singularity. *arXiv* **2008**, arXiv:0803.1988.
55. Cachazo, F.; Guevara, A. Leading Singularities and Classical Gravitational Scattering. *J. High Energy Phys.* **2020**, *2020*, 181. [[CrossRef](#)]
56. Guevara, A. Holomorphic Classical Limit for Spin Effects in Gravitational and Electromagnetic Scattering. *arXiv* **2017**, arXiv:1706.02314.
57. Guevara, A.; Ochirov, A.; Vines, J. Scattering of spinning black holes from exponentiated soft factors. *J. High Energy Phys.* **2019**, *2019*, 56. [[CrossRef](#)]
58. Menezes, G.; Sergola, M. NLO deflections for spinning particles and Kerr black holes. *arXiv* **2022**, arXiv:2205.11701.
59. Donoghue, J.F.; Menezes, G. Unitarity, stability, and loops of unstable ghosts. *Phys. Rev. D* **2019**, *100*, 105006. [[CrossRef](#)]
60. Donoghue, J.F.; Menezes, G. Gauge Assisted Quadratic Gravity: A Framework for UV Complete Quantum Gravity. *Phys. Rev. D* **2018**, *97*, 126005. [[CrossRef](#)]
61. Donoghue, J.F.; Menezes, G. On Quadratic Gravity. *arXiv* **2021**, arXiv:2112.01974.
62. Emond, W.T.; Moynihan, N. Scattering Amplitudes, Black Holes and Leading Singularities in Cubic Theories of Gravity. *J. High Energy Phys.* **2019**, *2019*, 19. [[CrossRef](#)]

63. Burger, D.J.; Emond, W.T.; Moynihan, N. Rotating Black Holes in Cubic Gravity. *Phys. Rev. D* **2020**, *101*, 084009. [[CrossRef](#)]
64. Veltman, M. Unitarity and causality in a renormalizable field theory with unstable particles. *Physica (Utrecht)* **1963**, *29*, 186. [[CrossRef](#)]
65. t' Hoof, G.; Veltman, M.J.G. Diagrammar. In *Particle Interactions at Very High Energies*; Speiser, D., Halzen, F., Weyers, J., Eds.; NATO Advanced Study Institutes, Series B; Plenum Press: New York, NY, USA, 1974; Volume 4, p. 177.
66. Rodenburg, J. Unstable Particles and Resonances. Master's Thesis, Utrecht University, Utrecht, The Netherlands, 2015.
67. Lang, J.-N.O. The Complex Mass Scheme, Gauge Dependence and Unitarity in Perturbative Quantum Field Theory. Master's Thesis, Würzburg University, Würzburg, Germany, 2013.
68. Denner, A.; Lang, J.N. The Complex-Mass Scheme and Unitarity in perturbative Quantum Field Theory. *Eur. Phys. J. C* **2015**, *75*, 377. [[CrossRef](#)]
69. Menezes, G. Generalized unitarity method for unstable particles. *arXiv* **2021**, arXiv:2111.11570.
70. Lee, T.D.; Wick, G.C. Negative Metric and the Unitarity of the S Matrix. *Nucl. Phys. B* **1969**, *9*, 209–243. [[CrossRef](#)]
71. Coleman, S. Acausality. In *Erice 1969: Ettore Majorana School on Subnuclear Phenomena*; Zicchici, A., Ed.; Academic Press: New York, NY, USA, 1970; p. 282.
72. Grinstein, B.; O'Connell, D.; Wise, M.B. The Lee-Wick standard model. *Phys. Rev. D* **2008**, *77*, 025012. [[CrossRef](#)]
73. Grinstein, B.; O'Connell, D.; Wise, M.B. Causality as an emergent macroscopic phenomenon: The Lee-Wick O(N) model. *Phys. Rev. D* **2009**, *79*, 105019. [[CrossRef](#)]
74. Donoghue, J.F.; Menezes, G. Arrow of Causality and Quantum Gravity. *Phys. Rev. Lett.* **2019**, *123*, 171601. [[CrossRef](#)] [[PubMed](#)]
75. Donoghue, J.F.; Menezes, G. Quantum causality and the arrows of time and thermodynamics. *Prog. Part. Nucl. Phys.* **2020**, *115*, 103812. [[CrossRef](#)]
76. Donoghue, J.F.; Menezes, G. Causality and gravity. *J. High Energy Phys.* **2021**, *2021*, 10. [[CrossRef](#)]
77. Cutkosky, R.E.; Landshoff, P.V.; Olive, D.I.; Polkinghorne, J.C. A non-analytic S matrix. *Nucl. Phys. B* **1969**, *12*, 281–300. [[CrossRef](#)]
78. Aglietti, U.G.; Anselmi, D. Inconsistency of Minkowski higher-derivative theories. *Eur. Phys. J. C* **2017**, *77*, 84. [[CrossRef](#)]
79. Anselmi, D.; Piva, M. A new formulation of Lee-Wick quantum field theory. *J. High Energy Phys.* **2017**, *2017*, 66. [[CrossRef](#)]
80. Anselmi, D.; Piva, M. Perturbative unitarity of Lee-Wick quantum field theory. *Phys. Rev. D* **2017**, *96*, 045009. [[CrossRef](#)]
81. Anselmi, D. Fakeons and Lee-Wick Models. *J. High Energy Phys.* **2018**, *2018*, 141. [[CrossRef](#)]
82. Anselmi, D.; Piva, M. Quantum Gravity, Fakeons and Microcausality. *J. High Energy Phys.* **2018**, *2018*, 21. [[CrossRef](#)]
83. Anselmi, D. Diagrammar of physical and fake particles and spectral optical theorem. *J. High Energy Phys.* **2021**, *2021*, 30. [[CrossRef](#)]
84. Johansson, H.; Nohle, J. Conformal gravity from gauge theory. *arXiv* **2017**, arXiv:1707.02965.
85. Johansson, H.; Mogull, G.; Teng, F. Unraveling conformal gravity amplitudes. *J. High Energy Phys.* **2018**, *2018*, 80. [[CrossRef](#)]
86. Azevedo, T.; Jusinskas, R.L.; Lize, M. Bosonic sectorized strings and the $(DF)^2$ theory. *J. High Energy Phys.* **2020**, *2020*, 82. [[CrossRef](#)]
87. Menezes, G. Color-kinematics duality, double copy and the unitarity method for higher-derivative QCD and quadratic gravity. *J. High Energy Phys.* **2022**, *2022*, 74. [[CrossRef](#)]
88. Bern, Z.; Carrasco, J.J.; Chiodaroli, M.; Johansson, H.; Roiban, R. The Duality Between Color and Kinematics and its Applications. *arXiv* **2019**, arXiv:1909.01358.
89. Bern, Z.; Carrasco, J.J.M.; Johansson, H. New relations for gauge-theory amplitudes. *Phys. Rev. D* **2008**, *78*, 085011. [[CrossRef](#)]
90. Johansson, H.; Ochirov, A. Color-Kinematics Duality for QCD Amplitudes. *J. High Energy Phys.* **2016**, *2016*, 170. [[CrossRef](#)]
91. Mastrolia, P.; Primo, A.; Schubert, U.; Bobadilla, W.J.T. Off-shell currents and color-kinematics duality. *Phys. Lett. B* **2016**, *753*, 242. [[CrossRef](#)]
92. Mafra, C.R.; Schlotterer, O.; Stieberger, S. Explicit BCJ Numerators from Pure Spinors. *J. High Energy Phys.* **2011**, *2011*, 92. [[CrossRef](#)]
93. Bjerrum-Bohr, N.E.J.; Bourjaily, J.L.; Damgaard, P.H.; Feng, B. Manifesting Color-Kinematics Duality in the Scattering Equation Formalism. *J. High Energy Phys.* **2016**, *2016*, 94. [[CrossRef](#)]
94. Du, Y.J.; Teng, F. BCJ numerators from reduced Pfaffian. *J. High Energy Phys.* **2017**, *2017*, 33. [[CrossRef](#)]
95. Du, Y.J.; Luo, H. On General BCJ Relation at One-loop Level in Yang–Mills Theory. *J. High Energy Phys.* **2013**, *2013*, 129. [[CrossRef](#)]
96. Yuan, E.Y. Virtual Color-Kinematics Duality: 6-pt 1-Loop MHV Amplitudes. *J. High Energy Phys.* **2013**, *2013*, 70. [[CrossRef](#)]
97. Boels, R.H.; Kniehl, B.A.; Tarasov, O.V.; Yang, G. Color-kinematic Duality for Form Factors. *J. High Energy Phys.* **2013**, *2013*, 63. [[CrossRef](#)]
98. Boels, R.H.; Isermann, R.S.; Monteiro, R.; O'Connell, D. Colour-Kinematics Duality for One-Loop Rational Amplitudes. *J. High Energy Phys.* **2013**, *2013*, 107. [[CrossRef](#)]
99. Bjerrum-Bohr, N.E.J.; Dennen, T.; Monteiro, R.; O'Connell, D. Integrand Oxidation and One-Loop Colour-Dual Numerators in $N = 4$ Gauge Theory. *J. High Energy Phys.* **2013**, *2013*, 92. [[CrossRef](#)]
100. Bern, Z.; Davies, S.; Dennen, T.; Huang, Y.t.; Nohle, J. Color-Kinematics Duality for Pure Yang–Mills and Gravity at One and Two Loops. *Phys. Rev. D* **2015**, *92*, 045041. [[CrossRef](#)]
101. Mogull, G.; O'Connell, D. Overcoming Obstacles to Colour-Kinematics Duality at Two Loops. *J. High Energy Phys.* **2015**, *2015*, 135. [[CrossRef](#)]

102. He, S.; Monteiro, R.; Schlotterer, O. String-inspired BCJ numerators for one-loop MHV amplitudes. *J. High Energy Phys.* **2016**, *2016*, 171. [[CrossRef](#)]
103. Yang, G. Color-kinematics duality and Sudakov form factor at five loops for $N = 4$ supersymmetric Yang–Mills theory. *Phys. Rev. Lett.* **2016**, *117*, 271602. [[CrossRef](#)]
104. He, S.; Schlotterer, O.; Zhang, Y. New BCJ representations for one-loop amplitudes in gauge theories and gravity. *Nucl. Phys. B* **2018**, *930*, 328. [[CrossRef](#)]
105. Borsten, L.; Jurco, B.; Kim, H.; Macrelli, T.; Saemann, C.; Wolf, M. Tree-Level Color-Kinematics Duality Implies Loop-Level Color-Kinematics Duality. *arXiv* **2021**, arXiv:2108.03030.
106. Chiodaroli, M.; Jin, Q.; Roiban, R. Color/kinematics duality for general abelian orbifolds of $N = 4$ super Yang–Mills theory. *J. High Energy Phys.* **2014**, *2014*, 152. [[CrossRef](#)]
107. Brandhuber, A.; Chen, G.; Johansson, H.; Travaglini, G.; Wen, C. Kinematic Hopf Algebra for BCJ Numerators in Heavy-Mass Effective Field Theory and Yang–Mills Theory. *arXiv* **2021**, arXiv:2111.15649.
108. Chen, G.; Du, Y.J. Amplitude Relations in Non-linear Sigma Model. *J. High Energy Phys.* **2014**, *2014*, 61. [[CrossRef](#)]
109. Kampf, K. The ChPT: Top-down and bottom-up. *arXiv* **2021**, arXiv:2109.11574.
110. Du, Y.J.; Fu, C.H. Explicit BCJ numerators of nonlinear sigma model. *J. High Energy Phys.* **2016**, *2016*, 174. [[CrossRef](#)]
111. Low, I.; Yin, Z. New Flavor-Kinematics Dualities and Extensions of Nonlinear Sigma Models. *Phys. Lett. B* **2020**, *807*, 135544. [[CrossRef](#)]
112. Donoghue, J.F.; Menezes, G. Ostrogradsky instability can be overcome by quantum physics. *Phys. Rev. D* **2021**, *104*, 045010. [[CrossRef](#)]
113. Salvio, A. Metastability in Quadratic Gravity. *Phys. Rev. D* **2019**, *99*, 103507. [[CrossRef](#)]
114. Britto, R.; Cachazo, F.; Feng, B. New recursion relations for tree amplitudes of gluons. *Nucl. Phys. B* **2005**, *715*, 499. [[CrossRef](#)]
115. Britto, R.; Cachazo, F.; Feng, B.; Witten, E. Direct proof of tree-level recursion relation in Yang–Mills theory. *Phys. Rev. Lett.* **2005**, *94*, 181602. [[CrossRef](#)] [[PubMed](#)]
116. Aoude, R.; Machado, C.S. The rise of SMEFT on-shell amplitudes. *J. High Energy Phys.* **2019**, *2019*, 58. [[CrossRef](#)]
117. Shadmi, Y.; Weiss, Y. Effective field theory amplitudes the on-shell way: Scalar and vector couplings to gluons. *J. High Energy Phys.* **2019**, *2019*, 165. [[CrossRef](#)]
118. Durieux, G.; Kitahara, T.; Shadmi, Y.; Weiss, Y. The electroweak effective field theory from on-shell amplitudes. *J. High Energy Phys.* **2020**, *2020*, 119. [[CrossRef](#)]
119. Arkani-Hamed, N.; Huang, T.-C.; Huang, Y.-T. Scattering amplitudes for all masses and spins. *arXiv* **2017**, arXiv:1709.04891.
120. Chung, M.-Z.; Kim, Y.-T.H.J.-W.; Lee, S. The simplest massive S-matrix: From minimal coupling to black holes. *J. High Energy Phys.* **2019**, *2019*, 156. [[CrossRef](#)]
121. Johansson, H.; Ochirov, A. Double copy for massive quantum particles with spin. *J. High Energy Phys.* **2019**, *2019*, 40. [[CrossRef](#)]
122. Henn, J.M.; Plefka, J.C. *Scattering Amplitudes in Gauge Theories*; Springer: Berlin, Germany, 2014.
123. Parke, S.J.; Taylor, T.R. An amplitude for n gluon scattering. *Phys. Rev. Lett.* **1986**, *56*, 2459. [[CrossRef](#)] [[PubMed](#)]
124. Plefka, J.; Shi, C.; Wang, T. Double copy of massive scalar QCD. *Phys. Rev. D* **2020**, *101*, 066004. [[CrossRef](#)]
125. Bern, Z.; Dennen, T.; Huang, Y.-t.; Kiermaier, M. Gravity as the square of gauge theory. *Phys. Rev. D* **2010**, *82*, 065003. [[CrossRef](#)]
126. Bern, Z.; Carrasco, J.J.M.; Johansson, H. Perturbative quantum gravity as a double copy of gauge theory. *Phys. Rev. Lett.* **2010**, *105*, 061602. [[CrossRef](#)] [[PubMed](#)]
127. Bern, Z.; Davies, S.; Nohle, J. Double-Copy Constructions and Unitarity Cuts. *Phys. Rev. D* **2016**, *93*, 105015. [[CrossRef](#)]
128. Bern, Z.; Carrasco, J.J.; Chen, W.M.; Johansson, H.; Roiban, R. Gravity Amplitudes as Generalized Double Copies of Gauge-Theory Amplitudes. *Phys. Rev. Lett.* **2017**, *118*, 181602. [[CrossRef](#)]
129. Carrasco, J.J.M.; Vazquez-Holm, I.A. Loop-Level Double-Copy for Massive Quantum Particles. *Phys. Rev. D* **2021**, *103*, 045002. [[CrossRef](#)]
130. Oxburgh, S.; White, C.D. BCJ duality and the double copy in the soft limit. *J. High Energy Phys.* **2013**, *2013*, 127. [[CrossRef](#)]
131. Ochirov, A.; Tourkine, P. BCJ duality and double copy in the closed string sector. *J. High Energy Phys.* **2014**, *2014*, 136. [[CrossRef](#)]
132. Borsten, L.; Jurco, B.; Kim, H.; Macrelli, T.; Saemann, C.; Wolf, M. Becchi-Rouet-Stora-Tyutin-Lagrangian Double Copy of Yang–Mills Theory. *Phys. Rev. Lett.* **2021**, *126*, 191601. [[CrossRef](#)] [[PubMed](#)]
133. Low, I.; Rodina, L.; Yin, Z. Double Copy in Higher Derivative Operators of Nambu-Goldstone Bosons. *Phys. Rev. D* **2021**, *103*, 025004. [[CrossRef](#)]
134. Brandhuber, A.; Chen, G.; Travaglini, G.; Wen, C. A new gauge-invariant double copy for heavy-mass effective theory. *J. High Energy Phys.* **2021**, *2021*, 47. [[CrossRef](#)]
135. Johnson, L.A.; Jones, C.R.T.; Paranjape, S. Constraints on a Massive Double-Copy and Applications to Massive Gravity. *J. High Energy Phys.* **2021**, *2021*, 148. [[CrossRef](#)]
136. Chiodaroli, M.; Gunaydin, M.; Johansson, H.; Roiban, R. Explicit Formulae for Yang–Mills–Einstein Amplitudes from the Double Copy. *J. High Energy Phys.* **2017**, *2017*, 2. [[CrossRef](#)]
137. Kawai, H.; Lewellen, D.C.; Tye, S.H.H. A relation between tree amplitudes of closed and open strings. *Nucl. Phys. B* **1986**, *269*, 1. [[CrossRef](#)]
138. Salvio, A. Quadratic gravity. *Front. Phys.* **2018**, *6*, 77. [[CrossRef](#)]

139. Chiodaroli, M.; Günaydin, M.; Johansson, H.; Roiban, R. Spontaneously broken Yang–Mills–Einstein supergravities as double copies. *J. High Energy Phys.* **2017**, *2017*, 64. [[CrossRef](#)]
140. Chiodaroli, M.; Günaydin, M.; Johansson, H.; Roiban, R. Gauged Supergravities and Spontaneous Supersymmetry Breaking from the Double Copy Construction. *Phys. Rev. Lett.* **2018**, *120*, 171601. [[CrossRef](#)]
141. Chiodaroli, M.; Günaydin, M.; Johansson, H.; Roiban, R. Non-Abelian gauged supergravities as double copies. *J. High Energy Phys.* **2019**, *2019*, 99. [[CrossRef](#)]
142. Donà, P.; Giaccari, S.; Modesto, L.; Rachwal, L.; Zhu, Y. Scattering amplitudes in super-renormalizable gravity. *J. High Energy Phys.* **2015**, *2015*, 38. [[CrossRef](#)]
143. Holdom, B. Photon-photon scattering from a UV-complete gravity QFT. *J. High Energy Phys.* **2022**, *2022*, 133. [[CrossRef](#)]
144. Brandhuber, A.; Spence, B.; Travaglini, G. Amplitudes in Pure Yang–Mills and MHV Diagrams. *J. High Energy Phys.* **2007**, *2007*, 88. [[CrossRef](#)]
145. Haber, H.E. Useful relations among the generators in the defining and adjoint representations of SU(N). *SciPost Phys. Lect. Notes* **2021**, *21*, 1. [[CrossRef](#)]
146. Dunbar, D.C.; Norridge, P.S. Calculation of graviton scattering amplitudes using string based methods. *Nucl. Phys. B* **1995**, *433*, 181–208. [[CrossRef](#)]
147. Bern, Z.; Grant, A.K. Perturbative gravity from QCD amplitudes. *Phys. Lett. B* **1999**, *457*, 23–32. [[CrossRef](#)]
148. Boulware, D.G.; Gross, D.J. Lee-Wick indefinite metric quantization: A functional integral approach. *Nucl. Phys. B* **1984**, *233*, 1–23. [[CrossRef](#)]
149. Arkani-Hamed, N.; Cachazo, F.; Cheung, C.; Kaplan, J. A Duality For The S Matrix. *J. High Energy Phys.* **2010**, *2010*, 20.
150. Hodges, A. Eliminating spurious poles from gauge-theoretic amplitudes. *J. High Energy Phys.* **2013**, *2013*, 135. [[CrossRef](#)]
151. Arkani-Hamed, N.; Bourjaily, J.L.; Cachazo, F.; Hodges, A.; Trnka, J. A Note on Polytopes for Scattering Amplitudes. *J. High Energy Phys.* **2012**, *2012*, 81. [[CrossRef](#)]
152. Arkani-Hamed, N.; Trnka, J. The Amplituhedron. *J. High Energy Phys.* **2014**, *2014*, 30. [[CrossRef](#)]
153. Arkani-Hamed, N.; Bai, Y.; He, S.; Yan, G. Scattering Forms and the Positive Geometry of Kinematics, Color and the Worldsheet. *J. High Energy Phys.* **2018**, *2018*, 96. [[CrossRef](#)]